

1 Reduced Cdc14 phosphatase activity impairs septation, hyphal differentiation and pathogenesis

2 and causes echinocandin hypersensitivity in *Candida albicans*

3 Kedric L. Milholland¹, Ahmed AbdelKhalek², Kortany M. Baker¹, Smriti Hoda¹, Andrew G. DeMarco¹,
4 Noelle H. Naughton¹, Angela N. Koeberlein¹, Gabrielle R. Lorenz¹, Kartikan Anandasothy¹, Antonio
5 Esperilla-Muñoz⁴, Sanjeev K. Narayanan², Jaime Correa-Bordes⁴, Scott D. Briggs^{1,3}, Mark C. Hall^{1,3,*}.

¹Department of Biochemistry, ²Department of Comparative Pathobiology, and ³Center for Cancer Research, Purdue University, West Lafayette, IN, USA.

⁸ ⁴Department of Biomedical Sciences, Universidad de Extremadura, Badajoz, Spain.

9

10 *Corresponding author – Email: mchall@purdue.edu

11

12 **Short Title:** Cdc14 contributes to *C. albicans* cell wall integrity and pathogenesis

13 ABSTRACT

14 The Cdc14 phosphatase family is highly conserved in fungi. In *Saccharomyces cerevisiae*, Cdc14
15 is essential for down-regulation of cyclin-dependent kinase activity at mitotic exit. However, this essential
16 function is not broadly conserved and requires a small fraction of normal Cdc14 activity. It remains
17 unclear what fungal Cdc14 functions require high Cdc14 activity. We identified an invariant motif in the
18 disordered C-terminal tail of fungal Cdc14 enzymes that is required for full enzyme activity. Mutation of
19 this motif reduced Cdc14 catalytic rate and provided a tool for studying the biological significance of high
20 Cdc14 activity. A *S. cerevisiae* strain expressing the reduced-activity hypomorphic mutant allele
21 (*cdc14^{hm}*) as the sole source of Cdc14 exhibited an unexpected sensitivity to cell wall stresses, including
22 chitin-binding compounds and echinocandin antifungal drugs. Sensitivity to echinocandins was also
23 observed in *Schizosaccharomyces pombe* and *Candida albicans* strains lacking *CDC14*, suggesting this
24 phenotype reflects a conserved function of Cdc14 orthologs in mediating fungal cell wall integrity. In *C.*
25 *albicans*, the orthologous *cdc14^{hm}* allele was sufficient to elicit echinocandin hypersensitivity and perturb
26 cell wall integrity signaling. It also caused striking abnormalities in septum structure and the same cell
27 separation and hyphal differentiation defects previously observed with *cdc14* gene deletions. Since hyphal
28 differentiation is important for *C. albicans* pathogenesis, we assessed the effect of reducing Cdc14
29 activity on virulence in *Galleria mellonella* and mouse models of invasive candidiasis. Partial reduction
30 in Cdc14 activity via *cdc14^{hm}* mutation severely impaired *C. albicans* virulence in both assays. Our results
31 reveal that high Cdc14 activity promotes fungal cell wall integrity and, in *C. albicans*, is needed to
32 orchestrate septation and hyphal differentiation, and for pathogenesis. Cdc14 may therefore be worth
33 future exploration as an antifungal drug target.

34 AUTHOR SUMMARY

35 Invasive fungal infections are a serious concern for the immune-compromised. Antifungal drugs
36 to treat invasive infections are limited and pathogens are developing resistance to them. Novel targets for
37 antifungal drug development are needed. In this study we developed a system to test if partial therapeutic
38 reduction in activity of a protein phosphatase called Cdc14 could reduce virulence of the opportunistic
39 human pathogen *Candida albicans*. This idea arose from prior studies in fungal pathogens of plants,
40 where Cdc14 was unexpectedly required for host infection through an unknown mechanism. We found
41 that successful *C. albicans* infections in two animal models of invasive candidiasis were dependent on
42 high Cdc14 activity. Moreover, we made the surprising observation that integrity of the *C. albicans* cell
43 wall is also dependent on high Cdc14 activity, with Cdc14-deficient cells becoming hypersensitive to cell
44 wall-targeted antifungal drugs. We conclude that even modest reduction in Cdc14 activity could have
45 therapeutic benefit for human fungal infections and possibly help overcome resistance to some antifungal
46 drugs. Cdc14 structure and specificity are unique among phosphatases and highly conserved in
47 pathogenic fungi, suggesting that highly selective inhibitors can be developed that would be useful
48 against a broad range of fungal pathogens.

49 INTRODUCTION

50 *CDC14* was originally identified in *Saccharomyces cerevisiae* as an essential gene required for
51 the final stage of nuclear division (1). The Cdc14 protein was subsequently characterized as a protein
52 phosphatase that fulfilled its essential function by terminating, and reversing the effects of, mitotic cyclin-
53 dependent kinase (Cdk) activity to trigger mitotic exit (2). *CDC14* is widely conserved in the major
54 eukaryotic lineages, with the exception of angiosperm plants (3–5), and Cdc14 catalytic domain structure,
55 activity and specificity are also broadly conserved (4,6–8). For example, human *CDC14* orthologs can
56 complement *cdc14* mutant phenotypes in *S. cerevisiae* and *Schizosaccharomyces pombe* (9,10).

57 Cdc14 is related to the dual-specificity phosphatase (DSP) subfamily of protein tyrosine
58 phosphatases (PTP), sharing the invariant HCX₅R catalytic motif and two-step catalytic mechanism
59 involving a covalent phospho-enzyme intermediate (11,12). Despite its clear evolutionary relationship to
60 the DSP and PTP families, Cdc14 evolved a very strong preference for phosphoserine sites followed by
61 the minimal sequence motif P-X-K (P-X-R to a lesser extent) in an ancestral eukaryote, making it
62 functionally a phosphoserine phosphatase. This unique specificity for a PTP family member arose from
63 an apparent duplication of the DSP domain, which created a novel substrate binding groove along a
64 domain interface adjacent to the active site (4,6,7). The tandem arrangement of DSP folds, and the
65 specificity it imparts, are signature features of Cdc14 enzymes across eukaryotes. The broad conservation
66 implies Cdc14 specificity must fill an essential niche in cellular regulation of most eukaryotic species that
67 cannot be provided by other prominent protein phosphatases. One hypothesis, based on work in the
68 oomycete *Phytophthora infestans*, is that Cdc14 co-evolved with eukaryotic flagella (5), and subsequent
69 studies have reported roles for Cdc14 enzymes in regulating aspects of cilia structure and function in
70 vertebrates, including human cells (13–15). The fungal subkingdom Dikarya, which includes most fungal
71 pathogens of plants and animals, represents a striking exception to the Cdc14-flagella correlation, as they
72 have strictly retained *CDC14* during evolution despite having lost flagella.

73 Within Dikarya, Cdc14 functional characterizations have been conducted in several species,
74 including the model yeasts *S. cerevisiae* and *S. pombe*. Interestingly, the originally described essential
75 function in terminating Cdk activity and triggering mitotic exit in *S. cerevisiae* is not widely conserved,
76 even in other ascomycetes. In fact, *CDC14* deletions in other fungal species often have modest impacts on
77 vegetative cell division (16–21). Moreover, we and others found that the essential function in *S.*
78 *cerevisiae* requires only a small fraction of natural Cdc14 expression (22–24). Cdc14 is an abundant
79 phosphatase in *S. cerevisiae*, with protein levels comparable to subunits of *PP2A* phosphatases (25). The
80 fact that a small fraction of expressed Cdc14 is sufficient for the essential function in *S. cerevisiae* implies
81 that the majority of Cdc14 is necessary for other important cellular functions.

82 Cdc14 has been linked to regulation of diverse biological processes in model fungi, including
83 centrosome duplication, mitotic spindle dynamics, chromosome segregation, DNA replication and repair,
84 polarized growth, autophagy, and response to osmotic and genotoxic stresses (26). The conservation of
85 many of these functions remains uncertain but it is now becoming clear that a highly conserved function
86 of fungal Cdc14 phosphatases is regulation of cytokinesis and septation at the end of the cell cycle. The *S.*
87 *pombe* Cdc14 ortholog, Clp1, does not regulate mitotic exit but plays multiple roles ensuring correct
88 cytokinesis and septation (20,27). Blocking Cdc14 nuclear export in *S. cerevisiae* allowed normal mitotic
89 exit regulation but resulted in cytokinesis defects (28). In the phytopathogenic fungi *Fusarium*
90 *graminearum* and *Magnaporthe oryzae*, *CDC14* deletion impaired septum formation and the coordination
91 between nuclear division and cytokinesis, leading to multi-nucleated conidial and hyphal compartments
92 (16,17). Similar septation defects were observed after *CDC14* deletion in another plant pathogen,
93 *Aspergillus flavus* (18). Finally, in the opportunistic human pathogen *Candida albicans*, *CDC14* deletion
94 caused defective cell separation after cytokinesis and septation, resulting in connected chains of cells
95 from failure to activate the Ace2 transcription factor (29). A number of Cdc14 substrates have been
96 identified and implicated in cytokinesis and septation regulation in *S. cerevisiae* and *S. pombe* (30) but the
97 relevant substrates remain unknown in most other fungal species.

98 Importantly, in studies of *CDC14* deletion-associated phenotypes in phytopathogenic fungi,
99 severe reductions in virulence were observed, even when vegetative growth was only marginally
100 impacted (16–18). The molecular mechanisms by which Cdc14 promotes plant infection are undefined. It
101 is unknown if *CDC14* is also important for virulence in animal fungal pathogens, although the *CDC14*
102 deletion in *C. albicans* impaired hyphal development, which is believed to be important for virulence
103 (31,32). Collectively, these reports suggest that one or more conserved Cdc14 functions in fungi is
104 generally important for host infection by pathogens.

105 In an attempt to better understand fungal Cdc14 functions unrelated to mitotic exit that require
106 high level expression, we sought a way to partially reduce Cdc14 activity *in vivo*. We focused on the
107 poorly conserved, and seemingly disordered, C-terminal tail, which is dispensable for phosphatase
108 activity and the essential mitotic exit function in *S. cerevisiae* (11). In some Cdc14 orthologs this region
109 has regulatory phosphorylation sites and elements that control cellular localization (28,33,34), but other
110 specific functions have not been described. Of note, the isolated ScCdc14 catalytic domain lacking the C-
111 terminal region exhibited reduced activity towards the generic phosphatase substrate *para*-nitrophenyl
112 phosphate (pNPP) in an early characterization of Cdc14 enzyme activity (11). We subsequently observed
113 a similar phenomenon with truncated Cdc14 enzymes from *F. graminearum* (16) and other fungal species
114 (our unpublished data), suggesting that the C-terminal region does make a conserved contribution to full
115 catalytic activity. Since the existing crystal structures of Cdc14 phosphatases lack the C-terminal tail
116 (6,7), it is unclear how this might occur, but it suggests that modulation of the C-terminus might allow
117 creation of reduced activity hypomorphic alleles that are otherwise normal and could be used to study the
118 functional importance of high level Cdc14 expression.

119 In this report, we identify a short, invariant motif in the disordered C-terminus of fungal Cdc14
120 enzymes that stimulates Cdc14 activity and is a likely target for *in vivo* Cdc14 regulation. We
121 characterized mutations in this motif in *S. cerevisiae* and *C. albicans*. The results revealed an unexpected
122 new role for Cdc14 in promoting fungal cell wall integrity and demonstrated that high level Cdc14
123 expression is critically important for *C. albicans* septation, hyphal development, and pathogenesis.

124 **RESULTS**

125 **A conserved motif in the fungal Cdc14 C-terminus is required for full catalytic activity.**

126 The observation that the isolated catalytic domains of multiple fungal Cdc14 orthologs have
127 reduced enzyme activity raised the possibility of creating hypomorphic mutants to test the importance of
128 full Cdc14 activity. Using *S. cerevisiae* Cdc14 (ScCdc14), we set out to identify regions of the ~200
129 amino acid C-terminal tail that specifically contribute to enzyme activity. We purified full length
130 ScCdc14(1-551), the catalytic domain truncation ScCdc14(1-374) and a truncation of intermediate length,
131 ScCdc14(1-449) (**Fig 1A and Fig S1A**) and compared activity under steady-state conditions. Consistent
132 with prior reports (11,16), ScCdc14(1-374) reaction rate towards pNPP was greatly reduced compared to
133 ScCdc14(1-551) (**Fig 1B**). ScCdc14(1-449) activity was nearly identical to ScCdc14(1-551),
134 demonstrating that the sequence between amino acids 374 and 449 is required for full activity. We used
135 ScCdc14(1-449) to represent full, or “wild-type”, activity in subsequent experiments. The same analysis
136 with a biologically-relevant phosphopeptide substrate derived from a known ScCdc14 substrate site in
137 Yen1 (36) revealed a similar large reduction in k_{cat} for ScCdc14(1-374) compared to ScCdc14(1-449),
138 indicating that the difference in activity is not substrate-dependent (**Fig 1C**).

139 A multiple sequence alignment of diverse fungal Cdc14 orthologs revealed a single, short
140 invariant sequence within the otherwise poorly conserved C-terminus (**Fig 1D**) that was not observed in
141 animal Cdc14 sequences (**Fig S2**). Part of this sequence, QPRK, strongly resembles the optimal substrate
142 recognition motif of Cdc14 enzymes, SPxK (“x” is preferentially a basic amino acid) (7,8,36), suggesting
143 it could influence catalysis by interacting with the active site as a pseudosubstrate. Furthermore, this motif
144 is within residues 374-449 required for full activity. We substituted Ala either for the Pro and Lys
145 residues, analogous to two critical positions for Cdc14 substrate recognition (7,8,36), or for the Gln, since
146 this residue would occupy the pSer binding pocket if the motif were acting as a pseudosubstrate. The
147 resulting ScCdc14(1-449^{QARA}) and ScCdc14(1-449^{APRK}) variants exhibited k_{cat} decreases similar to
148 ScCdc14(1-374) with both pNPP (**Fig 1E**) and phosphopeptide (**Fig 1F**) substrates. Mutation of QPRK

149 did not affect substrate specificity as activity was still dependent on the same major substrate features as
150 wild-type Cdc14 enzymes (**Fig S1B**). We conclude the QPRK motif makes a significant contribution to
151 enzyme turnover rate and is responsible for the observed rate difference between catalytic domain
152 truncations and full-length enzymes.

153 **QPRK motif mutation causes sensitivity to cell wall stress in *S. cerevisiae*.**

154 The strict conservation of the QPRK motif across the fungal kingdom suggests it is biologically
155 important. To characterize its biological significance, we generated a haploid *S. cerevisiae* strain
156 expressing the hypomorphic *cdc14^{QARA}* allele (hereafter called *cdc14^{hm}*) as the sole source of Cdc14 from
157 the natural *CDC14* locus using the *delitto perfetto* approach (37). In liquid culture, the mutant strain grew
158 at a similar rate to the wild-type parental strain at low cell density but slowed somewhat as cell density
159 increased and ultimately terminated at a slightly lower optical density (**Fig S3A**). Thus, the essential
160 mitotic exit function was not disrupted by the reduction in Cdc14 catalytic rate, consistent with our prior
161 observations that it requires a small fraction of normal Cdc14 activity (22). We performed agar plate
162 spotting assays in the presence of a variety of cellular stress conditions to determine if reducing Cdc14
163 activity sensitizes cells to stress. *cdc14^{hm}* colony size was slightly smaller than wild-type on untreated
164 control plates but otherwise grew similarly and *cdc14^{hm}* was no more sensitive than wild-type to
165 genotoxic, oxidative, and osmotic stresses (**Fig 2A** and **Fig S3B-D**). The temperature-sensitive *cdc14-3*
166 allele was previously shown to impart some sensitivity to calcofluor white (CFW), a chitin-binding
167 compound that causes cell wall stress (38). We confirmed this observation and found that *cdc14^{hm}*
168 exhibited strong sensitivity to CFW (**Fig 2B**) and another chitin-binding compound, Congo red (**Fig**
169 **S3E**). To determine if this sensitivity was unique to chitin binding chemicals we performed spotting
170 assays in the presence of echinocandin drugs, which cause cell wall stress by inhibiting synthesis of the
171 major cell wall polymer (1,3)- β -d-glucan (39). *cdc14^{hm}* was acutely sensitive to both micafungin and
172 caspofungin compared to wild-type (**Fig 2C-D**). *cdc14^{hm}* was also sensitive to growth at high temperature,
173 another condition that generates cell wall stress (40) (**Fig S3F**). Cell wall stress sensitivity was observed

174 when *cdc14^{hm}*, but not *CDC14*, was expressed from a CEN plasmid in a *cdc14Δ* background (**Fig S3G**).
175 Sensitivity in *cdc14^{hm}* was complemented by transformation with a CEN plasmid expressing wild-type
176 *CDC14* (**Fig S3H**), suggesting it is a recessive loss of function phenotype caused by the reduced activity.
177 Micafungin sensitivity was rescued in the presence of sorbitol, an osmotic stabilizer known to suppress
178 cell wall integrity defects (41), suggesting that reduced Cdc14 activity compromises cell wall integrity
179 (**Fig 2E**).

180 Cell wall damage activates the cell wall integrity (CWI) signaling pathway (42). Activation of the
181 CWI pathway can be monitored by immunoblotting for the phosphorylated CWI MAP kinase, Slt2. We
182 compared phospho-Slt2 levels in log phase wild-type and *cdc14^{hm}* cultures in the absence and presence of
183 micafungin. *cdc14^{hm}* showed a 3-fold increase in phospho-Slt2 in the absence of micafungin, but both
184 wild-type and *cdc14^{hm}* strains showed similar Slt2 activation after brief treatment with micafungin (**Fig**
185 **2F**). We also monitored expression of *FKS2*, which encodes a catalytic subunit of (1,3)- β -d-glucan
186 synthase that is induced by CWI signaling during cell wall stress (43–45). Consistent with the pSl2
187 result, *FKS2* transcript level was 2-fold higher in *cdc14^{hm}* compared to the isogenic wild-type strain in the
188 absence of micafungin (**Fig S3I**). These results are consistent with a cell wall integrity defect, but mostly
189 normal CWI signaling, in *cdc14^{hm}* *S. cerevisiae* cells.

190 **Cdc14-dependent cell wall stress hypersensitivity is conserved in *S. pombe* and *C. albicans***

191 To test if Cdc14-dependent sensitivity to cell wall stress is conserved in other fungal species, we
192 performed spotting assays with *CDC14* deletion strains of *S. pombe* and *C. albicans*. *S. pombe* *clp1Δ*
193 exhibited clear sensitivity to caspofungin, but not calcofluor white, presumably due to the lack of chitin in
194 *S. pombe* cell walls (46) (**Fig 3A**). *C. albicans* *cdc14Δ/Δ* exhibited strong sensitivity to calcofluor white,
195 caspofungin, and micafungin (**Fig 3B**). These observations suggest that Cdc14 makes a broadly conserved
196 contribution to fungal cell wall integrity.

197 We next tested if the QPRK motif functions similarly in *C. albicans* Cdc14 (CaCdc14) and if
198 mutating it is sufficient to cause cell wall stress sensitivity, as in *S. cerevisiae*. To our knowledge,

199 CaCdc14 has not been previously purified and characterized. We purified recombinant truncated
200 CaCdc14 (residues 1-427, which retains the QPRK motif), as full-length protein was insoluble, and
201 created a variant with Ala substitutions at the Gln, Pro, and Lys positions of the QPRK motif (**Fig S4A**).
202 CaCdc14(1-427) exhibited the same major substrate preferences as ScCdc14 and other Cdc14 orthologs
203 (**Fig S4B**), consistent with its identical active site composition (**Fig S2**). Steady-state kinetic analyses
204 with the Yen1 phosphopeptide substrate revealed a 6-fold reduction in k_{cat} for CaCdc14(1-427^{AARA})
205 compared to CaCdc14(1-427) (**Fig 3C**). Thus, the QPRK motif makes a similar, albeit somewhat weaker,
206 contribution to CaCdc14 phosphatase activity.

207 To study the biological significance of the QPRK motif in *C. albicans* we complemented
208 *cdc14Δ/Δ* with either *cdc14^{hm}-3xHA* (where *cdc14^{hm}* encodes the QPRK→AARA substitutions) or
209 *CDC14-3xHA* (**Fig S4C**). *cdc14^{hm}* growth rate was intermediate between the wild-type and *cdc14Δ/Δ*
210 strains, consistent with a partial loss of activity and function (**Fig S4D**). In agar plate spotting assays
211 *cdc14^{hm}/Δ* displayed hypersensitivity to a range of echinocandin concentrations, similar to *cdc14Δ/Δ*,
212 whereas *CDC14/Δ* behaved like the *CDC14/CDC14* wild-type parent strain (**Fig 3D-E**). Thus,
213 echinocandin hypersensitivity requires only a partial reduction in Cdc14 activity. As in *S. cerevisiae*,
214 hypersensitivity was specific to cell wall stress as *cdc14Δ/Δ* and *cdc14^{hm}/Δ* were mostly insensitive to
215 genotoxic, oxidative, and osmotic stress (**Fig S4E**).

216 **Reduced Cdc14 activity causes elevated CWI signaling and alters cell wall stress-induced gene
217 expression in *C. albicans***

218 We next tested if CWI signaling was altered in Cdc14-deficient *C. albicans* strains, similar to *S.*
219 *cerevisiae*. In *C. albicans*, the anti-p44/42 MAPK antibody used to detect the activated form of the CWI
220 MAP kinase produced several bands in our hands. We used the GRACE collection strains (47) for *MKC1*
221 (the *C. albicans* ortholog of *S. cerevisiae* *Slt2*) and the closely related MAP kinase *CEK1* to ensure we
222 were monitoring Mkc1 activation (**Fig S5**). In the absence of added stress, liquid cultures of both
223 *cdc14Δ/Δ* and *cdc14^{hm}/Δ* displayed an equal elevation in activating phosphorylation of Mkc1 compared to

224 *CDC14/CDC14* (**Fig 4A-B**). Interestingly, *CDC14*/ Δ cells displayed an intermediate elevation in
225 phospho-Mkc1 signal, suggesting that even *CDC14* haplo-insufficiency can cause some chronic cell wall
226 abnormality. The reason for this is unclear, but it suggests that CWI is particularly sensitive to Cdc14
227 activity level in *C. albicans*. In contrast to the basal state, when cultures were briefly challenged with
228 micafungin, Mkc1 activation was significantly lower in both *cdc14*/ Δ and *cdc14*^{hm}/ Δ compared to
229 *CDC14/CDC14* and *CDC14*/ Δ (**Fig 4A-B**). This suggests that Cdc14 activity may also play a role in
230 normal CWI pathway activation in response to certain cell wall stress signals.

231 To test if Cdc14 activity affects gene expression downstream of Mkc1 we used qRT-PCR to
232 measure transcript levels of several cell wall stress-responsive genes (48) in the absence and presence of
233 micafungin. Consistent with the phospho-Mkc1 immunoblotting results, *ECM331*, *PGA13*, and *PGA31*
234 transcripts were significantly elevated in *cdc14*/ Δ and/or *cdc14*^{hm}/ Δ strains compared to *CDC14/CDC14*
235 and *CDC14*/ Δ in the absence of micafungin, although *CRH11* showed no change (**Fig. 4C-F**).
236 Interestingly, after brief micafungin treatment *cdc14*/ Δ cells failed to induce expression of any of the
237 four genes and the fold-induction in *cdc14*^{hm}/ Δ was significantly reduced compared to wild-type strains.
238 This effect was not due to the genes already being maximally induced since three out of four transcript
239 levels were lower in micafungin-treated *cdc14*/ Δ and *cdc14*^{hm}/ Δ compared to *CDC14/CDC14* and
240 *CDC14*/ Δ . Thus, Cdc14 activity is important for expression of at least some cell wall stress-responsive
241 genes, and our results collectively imply a complex relationship between Cdc14 activity and cell wall
242 integrity signaling in *C. albicans* (see Discussion).

243 **Cdc14 deficiency impairs *C. albicans* septum assembly and cell separation.**

244 We used TEM to look for overt differences in cell wall structure between wild-type and Cdc14-
245 deficient *C. albicans* yeast form cells that could explain the observed cell wall integrity phenotypes. The
246 most striking difference was the structure of the septum in dividing cells. In *CDC14/CDC14* and
247 *CDC14*/ Δ cells the primary septum was uniformly visible as a bright, straight band bisecting the bud
248 neck, with thin layers of secondary septum on either side (**Fig 5A-B**), as expected (49). Relatively normal

249 primary septa were also observed in some *cdc14^{hm}*/ Δ and *cdc14Δ/Δ* cells, however we frequently observed
250 primary septa with abnormal morphologies in these strains that were never observed in wild-type cells
251 (**Fig 5C-D**). The primary septa were often discontinuous, non-linear, forked, or deviated from the bud
252 neck. Moreover, the secondary septa in *cdc14^{hm}*/ Δ and *cdc14Δ/Δ* were often thickened, and in some cases
253 appeared to lack primary septa altogether. These secondary septa were reminiscent of previously
254 described remedial septa that form in the absence of primary septum assembly (50). From the TEM
255 analysis we conclude that high Cdc14 activity is critical for proper septum assembly during cell division.

256 Previous characterization of *cdc14Δ/Δ* *C. albicans* revealed defects in separation of yeast form cells
257 following cell division, resulting in formation of large cell clumps (29). This phenotype was linked to
258 regulation of the Ace2 transcription factor that controls expression of cell separation genes following
259 cytokinesis and septation. In liquid cultures *cdc14^{hm}*/ Δ also formed large cell clumps that were
260 indistinguishable from *cdc14Δ/Δ*, whereas *CDC14/Δ* did not (**Fig 5E**). The clumps were dispersed by
261 sonication, consistent with normal completion of cytokinesis, but incomplete dissolution of septa. In
262 asynchronously growing cultures we detected similar reductions in the transcript levels of Ace2 target
263 genes in *cdc14^{hm}*/ Δ and *cdc14Δ/Δ* by qRT-PCR (**Fig S6**). This suggests that high Cdc14 activity is also
264 needed to fully activate Ace2. Thus, CaCdc14 appears to play critical roles in both the assembly and
265 dissolution of the septum during yeast form cell division. Septum defects could, in principle, contribute to
266 the impaired cell wall integrity of Cdc14-deficient cells.

267 **Reduced Cdc14 activity impairs *C. albicans* hyphal development and pathogenesis.**

268 *C. albicans* *cdc14Δ/Δ* was also previously reported to be defective in hyphal differentiation and
269 invasive growth on agar plates (29). We therefore tested if *cdc14^{hm}*/ Δ also exhibits these phenotypes. On
270 Spider medium plates, *cdc14Δ/Δ* and *cdc14^{hm}*/ Δ were completely unable to develop filamentous colonies
271 and exhibited very limited agar invasion (**Fig 6A**). Microscopic analysis of cells extracted from the Spider
272 agar after washing of the plate surface revealed that even invasive cells exhibited a severe reduction in the
273 number and length of hyphae compared to strains with wild-type *CDC14* (**Fig 6B**). Similar lack of

274 invasion and formation of hyphae by *cdc14Δ/Δ* and *cdc14^{hm}/Δ* were also observed on YPD-serum agar
275 plates (**Fig S7A-B**). In liquid cultures, hyphal differentiation differences between the strains were more
276 subtle. Both *cdc14Δ/Δ* and *cdc14^{hm}/Δ* exhibited hyper-polarized growth consistent with hyphae, but at two
277 hours after serum induction their elongated cells were shorter on average and displayed more
278 pseudohyphal character than those of the wild-type *CDC14* strains (**Fig S7C**). We conclude that normal
279 hyphal development also requires high *CDC14* activity.

280 Hyphal differentiation is thought to be important for *C. albicans* virulence (32), suggesting that
281 reduced Cdc14 activity might compromise pathogenesis. We tested this idea in two established animal
282 models of invasive candidiasis, the larvae of the wax moth *Galleria mellonella* (51–54), and
283 immunosuppressed mice (55). In *G. mellonella*, *cdc14Δ/Δ* and *cdc14^{hm}/Δ* exhibited dramatically reduced
284 virulence compared to *CDC14/CDC14* and *CDC14/Δ* (**Fig 7A**). In mice the virulence defect associated
285 with reduced Cdc14 was even more dramatic. An initial titration of fungal dose revealed *cdc14Δ/Δ* to be
286 almost completely avirulent even at the highest fungal titer (**Fig S8A-B**). At the minimum
287 *CDC14/CDC14* dose required for complete mortality, *cdc14^{hm}/Δ* failed to kill any mice and, surprisingly,
288 *CDC14/Δ* resulted in 50% mortality, killing only the female mice, suggesting *CDC14* heterozygosity is
289 sufficient to impact virulence and that there may be a gender bias in sensitivity to Cdc14 deficiency (**Fig**
290 **7B**).

291 Histological analysis of mouse organs following infection revealed extensive colonization by
292 predominantly hyphal cells of *CDC14/CDC14* and *CDC14/Δ* strains, resulting in inflammation and
293 necrosis, as expected (**Fig 7C-E and Fig. S8C**). In contrast, minimal colonization and necrosis were
294 observed after infection by *cdc14^{hm}/Δ* and *cdc14Δ/Δ* strains and the rare fungal cells that were detected
295 were almost completely yeast form, consistent with the hyphal differentiation defects observed on agar
296 plates. In mice infected with wild-type *C. albicans*, organs like the liver and lungs showed evidence of
297 shock prior to appearance of fungal cells. Lesions consistent with shock included endothelial leakage
298 characterized by edema fluid, multifocal hemorrhage and congestion, and occasional intravascular
299 microthrombi (**Fig 7D-E**). These were not observed in the organs of mice infected with *cdc14^{hm}/Δ* or

300 *cdc14Δ/Δ*, raising the possibility that Cdc14 promotes secretion of soluble factors that contribute to
301 vascular damage. These results show that high Cdc14 activity is critically important for *C. albicans*
302 pathogenesis.

303 **DISCUSSION**

304 Our results identify Cdc14 phosphatase as a novel virulence factor in *C. albicans* and reveal a
305 new and conserved contribution of Cdc14 to fungal cell wall integrity. Importantly, partial loss of Cdc14
306 activity through mutation of a conserved catalytic enhancer element in the disordered C-terminal region
307 was sufficient to render *C. albicans* hypersensitive to cell wall stress, and impair septation, hyphal
308 development, and pathogenesis. Since *C. albicans* virulence depends on hyphal differentiation (31,32),
309 the pathogenesis phenotype could be explained by the hyphal defect of Cdc14-deficient strains. However,
310 CaCdc14 function in septation and cell wall integrity may contribute to virulence as well, a possibility
311 that will require future testing. We speculate that the observed cell wall integrity and septation defects
312 reflect a general importance of high level Cdc14 expression across fungi.

313 **Cdc14 importance for fungal septation**

314 Cdc14 has been implicated in regulation of septation and cell separation previously. In *S.*
315 *cerevisiae* Cdc14 promotes delivery of the chitin synthase Chs2, which synthesizes the primary septum,
316 to the bud neck after completion of mitosis (56). It also regulates actomyosin ring assembly (57) and the
317 ingression progression complex that coordinates actomyosin ring contraction and membrane ingression
318 with Chs2-dependent septum assembly (58–60). Mutations in the Mitotic Exit Network, which activates
319 ScCdc14, lead to septum structural defects (60). In the phytopathogenic fungi *Fusarium graminearum*,
320 *Magnaporthe oryzae*, and *Aspergillus flavus*, *CDC14* deletion reduces the number of septa in conidia and
321 vegetative hyphae and in *M. oryzae* perturbs correct localization of appressoria-delimiting septa (16–18).
322 Despite the evidence that Cdc14 is important for normal septation, our results appear to be the first to
323 show that Cdc14 deficiency causes structural defects in primary septa. Cdc14 is also important for
324 dissolving septa to allow cell separation. ScCdc14 dephosphorylates and activates Ace2 to induce cell
325 separation genes (61,62), and preventing ScCdc14 nuclear export or reducing Cdc14 level via inducible
326 degradation resulted in cell separation failure (22,28). Cdc14 is also needed to activate Ace2 to promote
327 cell separation in *C. albicans* (29). Septation and cell separation defects could be a primary cause of the

328 cell wall stress sensitivity observed in Cdc14-deficient *C. albicans*, although direct evidence of such a
329 causal relationship is still missing.

330 **A novel role for fungal Cdc14 in cell wall integrity and stress signaling**

331 In addition to causing a cell wall structural defect, our results suggest that Cdc14 deficiency
332 impacts CWI signaling in *C. albicans* in a complex way. Despite the elevated CWI pathway activation in
333 unstressed Cdc14-deficient strains (including heterozygous *CDC14*/ Δ), *cdc14* Δ / Δ and *cdc14*^{hm}/ Δ exhibited
334 reduced stimulation of phospho-Mkc1 following micafungin treatment. This suggests that Cdc14
335 deficiency both causes cell wall damage and also plays a role in activating the response to this damage.
336 Consistent with this idea, Cdc14-deficient strains displayed modest up-regulation of a subset of known
337 cell wall stress-responsive genes in the absence of added stress (in line with elevated phospho-Mkc1) but
338 were defective in stimulating expression of these genes in response to micafungin exposure. The extent of
339 this defect correlated with the severity of Cdc14 deficiency; *cdc14* Δ / Δ showed no micafungin-stimulated
340 expression of the four cell wall stress-responsive genes we tested. These results are somewhat difficult to
341 reconcile but are most consistent with Cdc14 influencing CWI signaling at steps upstream and
342 downstream of Mkc1. Consequently, the cell wall stress sensitivity phenotype could be explained by a
343 Cdc14-dependent cell wall structural defect, a deficiency in the CWI signaling response to the cell wall
344 defect, or both. The fact that *CDC14*/ Δ cells exhibited increased basal phospho-Mkc1 but normal CWI
345 signaling and transcriptional response after micafungin treatment reinforces the idea that Cdc14 functions
346 in multiple capacities to promote cell wall integrity that are differentially sensitive to its activity level. We
347 surveyed a small subset of cell wall stress-responsive genes, and a complete picture of how Cdc14
348 impacts the response to cell wall stress will ultimately require global approaches like RNA-seq.

349 Cdc14 was previously linked to several fungal stress pathways. *S. pombe* Clp1 and ScCdc14 are
350 released from the nucleolus and activated in response to genotoxic stress (63–65). A global phosphatase
351 and kinase interaction network analysis revealed multiple interactions of ScCdc14 with stress signaling
352 MAP kinases (38) and other studies have reported connections between Cdc14 and the osmotic stress

353 response mediated by the Hog1 MAP kinase (66,67). In the phytopathogen *A. flavus*, a *cdc14Δ* strain
354 exhibited growth delays in the presence of chitin-binding compounds and osmotic stress (18). In the
355 entomopathogen *Beauveria bassiana*, *cdc14Δ* displayed modest sensitivity to multiple stresses, including
356 the chitin-binding Congo red (19). These studies imply that fungal Cdc14 may play diverse roles in
357 facilitating fungal stress responses, although we emphasize that *cdc14^{hm}/Δ* *C. albicans* with partial loss of
358 Cdc14 activity exhibited a very specific sensitivity to cell wall stress. An area for future investigation will
359 be determining if the cell wall stress hypersensitivity of Cdc14-deficient strains is related to the virulence
360 defect. Specific mutations that affect Cdc14 function in cell wall integrity would facilitate this and could
361 be enabled by a thorough understanding of Cdc14 regulation during cell division, in response to cell wall
362 stress, and during hyphal development.

363 **The significance of Cdc14 activity level and the C-terminal catalytic enhancer motif**

364 Our results reinforce the fact that different functions of Cdc14 require different levels of activity.
365 In *S. cerevisiae* the essential mitotic exit function requires a small fraction of normal Cdc14 activity (22).
366 Why would functions in cytokinesis and cell wall integrity require much higher Cdc14 activity? In *S.*
367 *cerevisiae* the essential function is fulfilled by nuclear Cdc14 (28) whereas cytokinesis functions require
368 cytoplasmic Cdc14 generated by the Mitotic Exit Network kinases (68). One possibility is that
369 cytoplasmic functions require more enzyme because of the greater volume relative to the nucleus, which
370 effectively dilutes Cdc14 concentration. In *C. albicans* Cdc14 localization is also cell-cycle regulated. It
371 is primarily nuclear prior to mitosis, then appears at the spindle pole bodies during early mitosis, and
372 finally becomes cytoplasmic and localizes to the bud neck in late mitosis (29). A second possibility is that
373 the mitotic exit function requires minimal activity to trigger a positive feedback system (69), whereas the
374 cytokinesis, septation, and cell wall integrity functions depend on bulk substrate dephosphorylation that
375 necessitates higher Cdc14 concentration. A third possibility is that Cdc14 has high affinity for mitotic exit
376 substrates that must be dephosphorylated relatively early after Cdc14 activation and lower affinity for
377 substrates involved in later processes like cytokinesis and septation, resulting in a need for higher Cdc14

378 activity to achieve their dephosphorylation. There is evidence that substrate affinity does influence the
379 order of Cdc14 substrate dephosphorylation during mitotic exit (70), providing some support for this
380 possibility.

381 Regardless of the true explanation, it appears clear that Cdc14 activity levels in *C. albicans* and *S.*
382 *cerevisiae* are physiologically important. Even heterozygous *CDC14/cdc14Δ* cells exhibited some
383 phenotypes, most notably the reduction in virulence in the mouse infection assay. We speculate that the
384 invariant QPRK motif in the C-terminus of fungal Cdc14 enzymes exists to provide a mechanism for
385 regulating Cdc14 activity level around a critical threshold. Although the need for this mechanism is still
386 unclear, results from both *S. cerevisiae* and *S. pombe* support its existence. A C-terminal Cdk
387 phosphorylation site in ScCdc14 was previously shown to inhibit enzyme activity by an unknown
388 mechanism (33). This site happens to be adjacent to the QPRK motif and also appears to be essentially
389 invariant in fungi (although its exact position relative to QPRK varies, see alignment in Fig. 1D). In *S.*
390 *pombe* Clp1 phosphorylation by Cdk1 at C-terminal sites (including the one adjacent to its QPRK motif)
391 also reduces enzymatic activity and is required for normal kinetics of mitotic progression (34). Thus, it
392 appears likely that phosphoregulation of QPRK motif function is a mechanism for controlling overall
393 Cdc14 activity level in fungal species. It will be interesting to test if phosphorylation adjacent to the
394 QPRK motif of CaCdc14 also regulates enzyme activity and if dephosphorylation is required to promote
395 CaCdc14 function in septation, hyphal development, and the response to cell wall stress.

396 **CaCdc14 substrates important for septation, CWI, and hyphal development**

397 While a number of substrates of ScCdc14 and SpCdc14 involved in regulation of cytokinesis
398 and/or septation have been identified (71–74), it remains unknown what substrates of CaCdc14 must be
399 dephosphorylated to promote normal septum assembly, cell wall integrity, and hyphal differentiation.
400 Understanding how Cdc14 influences these processes will require identification of the relevant direct
401 substrates. Evidence suggests that Ace2 is a CaCdc14 substrate likely related to the observed cell
402 separation defects in Cdc14-deficient strains (29). A previous proteomic study of CaCdc14 interacting

403 proteins and candidate substrates did not identify proteins with obvious connections to septum assembly
404 but did identify Ace2, the chitinase Cht4, and a couple components of the actomyosin contractile ring
405 (75), although these were not validated as substrates. Thus, our current knowledge of Cdc14 substrates in
406 *C. albicans* is very limited.

407 **Cdc14 may have potential as an antifungal drug target**

408 The observation that partial reduction in Cdc14 activity severely impairs pathogenesis in animal
409 models of invasive candidiasis suggests that Cdc14 might be a useful antifungal drug target where even
410 modest therapeutic inhibition of activity could successfully combat infections. Moreover, the fact that
411 reduced Cdc14 activity sensitizes *C. albicans* to echinocandin drugs raises the possibility that Cdc14
412 inhibitors could be valuable for combating clinical echinocandin resistance. We argued previously that the
413 Cdc14 active site should be amenable to specific inhibitor development (4). High resolution structural
414 information on substrate recognition by the fungal Cdc14 active site is available (7), and despite sharing a
415 common catalytic mechanism with PTPs, Cdc14 possesses a strict and unusual substrate specificity that
416 could be mimicked for effective and highly selective inhibitor development. In animals, deletion of
417 CDC14 has little impact on cell division and development (76–78) and the possibility of successful
418 therapeutic intervention by partial inhibition of Cdc14 activity further minimizes the likelihood of
419 deleterious effects on human cells. The Cdc14 active site region is invariant across the fungal kingdom
420 (4) and therefore inhibitors developed to target CaCdc14 would likely be effective at inhibiting Cdc14
421 orthologs from many other pathogens. For this reason, it will be useful in the future to determine if Cdc14
422 is similarly required for infection by other human pathogens.

423 **METHODS**

424 *Strain and plasmid construction.* All plasmids and strains used in this study are listed in
425 Supplementary Tables S1 and S2, respectively. All engineered strains were confirmed by PCR and DNA
426 sequencing. *S. cerevisiae* strain YKA1038 expressing *cdc14^{hm}* in W303 background was created using the
427 *delitto perfetto* approach exactly as described (37). The plasmid shuffle *cdc14Δ* strain HCY109 and the
428 pRS314 plasmid expressing *CDC14* from its natural promoter were gifts from Dr. Harry Charbonneau,
429 Purdue University. To replace wild-type *CDC14* in HCY109, cells were transformed with pRS314
430 expressing either *cdc14^{hm}* or *CDC14* followed by selection on 5-FOA to eliminate the URA3-based
431 pRS316-*CDC14* plasmid. *C. albicans* strain JC2712 was created by integration of *CaURA3* at the
432 *NEUT5L* locus in CAI4. JC2711 was created by deletion of both copies of *CDC14* using the URA blaster
433 method (79) followed by integration of *CaURA3* at the *NEUT5L* locus. *C. albicans* complementing
434 strains expressing a single-copy of wild-type *CDC14-3xHA* (JC2721) or *cdc14^{hm}-3xHA* (HCAL102) were
435 created by transformation of a *SalI* and *EcoRV* fragment of pJC347 or pHLP661, respectively, into JC8
436 (CAI4 *cdc14Δ/Δ*) and selecting on SD-URA medium. To create pJC347, the 3' UTR of *CDC14* (+250 to
437 +536 bp after the STOP codon) was PCR-amplified with the addition of *SacI* and *EcoRV* sites to the 5'
438 and 3' ends, respectively, and cloned into *SacI* and *EcoRV*-digested pFA-URA3 (80) to generate pFA-
439 URA3-*CDC14*utr. Then, a synthetic DNA with *SalI* and *BamHI* sites added to the 5' and 3' ends,
440 respectively, containing 400bp of *CDC14* promoter, the *CDC14-3xHA* ORF and a 3-UTR with the first
441 249 bp after the STOP codon of the *CDC14* gene was cloned into the *SalI* and *BamHI* sites on pFA-
442 URA3-*CDC14*utr. To create pHLP661, the *cdc14^{hm}* mutation (encoding ⁴¹⁴QPRK → ⁴¹⁴AAKA
443 substitutions) was generated with the QuikChange Lightning site-directed mutagenesis kit (210518,
444 Agilent) using pJC347 as the template and confirmed by DNA sequencing. *yap1Δ* and *hog1Δ* strains were
445 obtained from the *S. cerevisiae* haploid deletion library (Horizon Discovery). The *yen1Δ* *mus81Δ* *S.*
446 *cerevisiae* strain was a gift from Dr. Lorraine Symington, Columbia University. *S. pombe* strains were a

447 gift from Dr. Kathleen Gould, Vanderbilt University. The *cdc14-3* strain was a gift from Dr. Michael
448 Weinreich, Van Andel Research Institute.

449 *E. coli* expression plasmids for purification of recombinant Cdc14 enzymes were generated using
450 the Gateway cloning system (Invitrogen). *S. cerevisiae* *CDC14* coding sequence was amplified by PCR
451 from an existing plasmid. *C. albicans* *CDC14* coding sequence was amplified from a cDNA preparation
452 to avoid its intron. Both were cloned into the pENTR/D-TOPO entry vector and then transferred to
453 pDEST17 destination vector following the provided instructions for expression with an N-terminal 6xHis
454 tag. Mutations to the QPRK motif of both were generated by QuikChange mutagenesis. Full coding
455 sequences for all plasmids were verified by DNA sequencing.

456 *Cell culture.* Liquid *S. cerevisiae* and *C. albicans* cultures were grown in YPD medium (10 g/L
457 yeast extract, 20 g/L peptone, 20 g/L glucose). YPD was supplemented with 40 mg/L adenine (YPAD)
458 for *S. cerevisiae* W303 strains. Cultures were grown at 30°C with shaking at 225 rpm. *S. pombe* strains
459 were grown in YES (5 g/L yeast extract, 30 g/L glucose, 225 mg/L adenine, histidine, leucine, uracil, and
460 lysine) at 30°C with shaking at 225 rpm. *E. coli* were grown in 2xYT (16 g/L tryptone, 10 g/L yeast
461 extract, and 5 g/L NaCl) at 37°C with shaking at 225 rpm. Agar was added to 20% (w/v) for growth on
462 solid medium. For agar plate spotting assays, single colonies were grown to saturation. Strains were
463 serially diluted in 8-fold steps starting from OD₆₀₀ = 1.0 and 5 µL of four consecutive dilutions were
464 spotted on plates and grown at 30°C for 3-5 days. *C. albicans* *cdc14Δ/Δ* cultures were diluted one less
465 time than other strains and spots therefore correspond to 8-fold higher absorbance; this was necessary to
466 normalize colony density on untreated control plates. For hyphal induction on solid medium, *C. albicans*
467 strains were streaked for single colonies on Spider media plates (10 g/L beef broth, 10 g/L mannitol, 2 g/L
468 K₂HPO₄, 20 g/L agar) or YPD plates supplemented with 10% fetal bovine serum (FBS) (Atlanta
469 Biologicals, S11550) and grown at 37°C for 5 days. For liquid hyphal induction, strains were grown
470 overnight to saturation at 30 °C and diluted to an OD₆₀₀ = 0.1 in pre-warmed 37 °C YPD containing 10%
471 FBS. Cultures were then incubated at 37°C with shaking at 225 rpm.

472 *Immunoblotting.* Total protein extracts were prepared as described (81,82) with subtle
473 modifications. Briefly, 8 mL of mid-log phase cells were treated with 10% trichloroacetic acid and
474 pelleted by centrifugation. Cell pellets were washed with 10 mL 70% ethanol and 2x with 1 mL water,
475 then re-suspended in 1 mL 0.2 M NaOH and incubated 10 min on ice. Cells were pelleted, resuspended in
476 160 x OD₆₀₀ µl loading dye (120 mM Tris-HCl pH 6.8, 4% sodium dodecyl sulfate, 0.02% bromophenol
477 blue, 20% glycerol), heated at 95°C for 10 min, and lysates clarified by centrifugation at 16,000 x g.
478 Proteins were separated on 10% tris-glycine SDS-PAGE gels, transferred to 0.45 µm nitrocellulose
479 membranes (Bio-Rad) and probed overnight at 4 °C with mouse anti-HA (1:5,000; Sigma-Aldrich,
480 12CA5), rabbit anti-PSTAIR (1:5,000; Millipore-Sigma, 06-923), rabbit anti-p44/42 MAPK (1:2,500;
481 Cell Signaling Technology, 9102) or rabbit anti-G6PDH (1:5,000; Sigma-Aldrich, A9521). Secondary
482 anti-mouse and anti-rabbit antibodies conjugated to horseradish peroxidase were from Jackson
483 ImmunoResearch (115-035-003 or 111-035-003) and used at 1:10,000 dilution for 60 min at 4 °C.
484 Immunoblots were developed using Clarity Western ECL Substrate (Bio-Rad, 170-5060) and imaged on a
485 ChemiDoc MP multimode imager (Bio-Rad).

486 *Protein purification.* 6xHis-Cdc14 enzymes were purified from *E. coli* as previously described
487 (4).

488 *Enzyme kinetics.* Activities towards varying concentrations of pNPP and synthetic
489 phosphopeptides were assayed as previously described (4).

490 *qRT-PCR.* Cells were grown to mid-log phase (OD₆₀₀ ~ 0.8) in YPD and, where indicated, treated
491 with 50 ng/mL micafungin for 1 hour prior to RNA extraction. RNA was isolated and purified using acid
492 phenol as described (83,84). Reverse transcription was performed using All-in-One 5X RT MasterMix
493 (ABM, G592). Primer Express 3.0 software was used to design primers and qRT-PCR was performed as
494 previously described (83,84) with at least three biological replicates. Data were analyzed using the
495 comparative *C_T* method (2^{-ΔΔCT}). Internal controls were *RDN18* (18S rRNA) for *C. albicans* and *ACT1* for
496 *S. cerevisiae*. All samples were normalized to an untreated wild-type strain.

497 *Galleria mellonella* infection assays. Larvae of *G. mellonella* were purchased from
498 waxworms.net (St. Marys, OH) and infection assays were performed similar to previous reports (52,85).
499 Upon arrival, larvae were held at room temperature in the dark, without food for 24 hours before
500 injection. *C. albicans* strains were grown to saturation in YPD and cells washed three times with PBS,
501 sonicated for 10 seconds, and counted using a Luna-FL automated cell counter (Logos Biosystems).
502 Larvae (n ≥ 40 per strain) of similar size and color were injected with 6 µL of 2x10⁵ cells into their lower
503 left proleg using a Hamilton syringe. An additional group was injected with PBS to serve as a negative
504 control. Injected larvae were incubated in petri dishes at 37°C in the dark for 5 days. Death was measured
505 every 24 hours based on the ability of the larvae to flip over after being placed on their backs. Survival
506 data was plotted using the Kaplan-Meier survival curve and statistical analysis was performed using a
507 log-rank Mantel-Cox test.

508 *Mouse infection assay*. BALB/c mice (n=8 per strain, 4 males and 4 females, 5-week-old) were
509 acclimatized for 7 days upon arrival. On days 8 and 11, mice were rendered neutropenic by
510 intraperitoneal (IP) doses of cyclophosphamide; 150 mg/kg on day 8 and 100 mg/kg on day 11. On day
511 12, 5 x 10⁵ CFUs of a *C. albicans* strain (measured using a hemocytometer after staining with 0.4%
512 trypan blue to rule out dead cells) in 0.2 mL PBS were administered via IP injection. An additional group
513 received cyclophosphamide but was not infected to serve as a negative control. Mice were monitored for
514 morbidity every 6 hours and were euthanized upon showing severe signs of illness, including weight loss
515 (>20%), dyspnea, unresponsiveness, staggered gait, and inability to eat. On day 19, surviving mice were
516 humanely euthanized through CO₂ inhalation. Lungs, liver, spleen, and kidneys were collected from
517 euthanized mice for histopathology. Survival data were plotted using the Kaplan-Meier survival curve and
518 statistical analysis was performed using a log-rank Mantel-Cox test. Selection of 5 x 10⁵ CFUs of each *C.*
519 *albicans* strain was based on a pilot study performed using different doses (5 x 10⁶ to 1 x 10⁴ CFUs) of
520 both wild-type and *cdc14Δ/Δ* strains (**Fig S8A-B**).

521 *Histopathology*. Lungs, kidneys, and livers from euthanized mice were formalin-fixed, and
522 transferred to 70% ethanol on the next day. Tissues were embedded in paraffin, sectioned, and stained

523 with hematoxylin and eosin (H&E) at the Purdue Histology Research Laboratory for histopathological
524 examination. Tissues were examined by a board-certified veterinary anatomic pathologist, histological
525 features were evaluated, and representative tissue sections were photographed. Fungal pathogens were
526 visualized and evaluated for morphology using periodic acid Schiff (PAS) staining.

527 *Transmission electron microscopy.* Samples were prepared based on a previously published
528 protocol (86) with minor modifications. Day 1: Samples were fixed by adding cell culture to an equal
529 volume of 5% glutaraldehyde in 0.1 M sodium cacodylate buffer. After five min cells were pelleted by
530 centrifugation, resuspended in 2.5% glutaraldehyde in the same buffer, and fixed overnight at 4 °C. Day
531 2: Cells were rinsed and resuspended in 2% aqueous potassium permanganate for one hour, then rinsed
532 until the solution cleared. Cells were then embedded in agarose, *en bloc* stained in 1% aqueous uranyl
533 acetate for one hour and rinsed. Day 3: Samples were dehydrated with a graded series of ethanol, then
534 transferred into a 2:1 mixture of ethanol and LR White resin and rotated for 2 hours. They were then
535 transferred into a 1:1 mixture of ethanol and LR White resin and rotated overnight. Day 4: Samples were
536 moved into pure LR White resin, rotated for two hours, then placed under house vacuum. The resin was
537 changed three times throughout the day and the samples remained under vacuum overnight. Day 5:
538 Samples were embedded in LR White resin in gelatin capsules and polymerized at 60 °C for 24 hours.
539 Thin sections were cut on a Leica UC6 ultramicrotome and stained with 4% uranyl acetate and lead
540 citrate. Images were acquired on a FEI Tecnai T12 electron microscope equipped with a tungsten source
541 operated at 80 kV.

542 **FIGURE LEGENDS**

543 **Figure 1. A conserved motif in Cdc14's disordered C-terminal tail is required for full catalytic**
544 **activity. (A)** Domain map of Cdc14. DSPn and DSPc are the N- and C-terminal dual-specificity
545 phosphatase domains, respectively. CX₅R is the invariant PTP family catalytic motif. Sites of truncations
546 and the invariant QPRK motif are indicated in the disordered C-terminus following DSPc. **(B)** Steady-
547 state kinetic analyses with full length ScCdc14(1-551) and the indicated truncation variants towards pNPP
548 yielded k_{cat} values of 0.91 (1-551), 0.80 (1-449) and 0.04 (1-374) sec⁻¹. **(C)** Same as (B) with
549 phosphopeptide substrate HT[pS]PIKSIG, yielding k_{cat} values of 0.64 (1-449) and 0.01 (1-374) sec⁻¹. **(D)**
550 Multiple sequence alignment of fungal Cdc14 orthologs from the indicated species was generated by
551 Clustal Omega using default settings. Only a portion of the C-terminal region showing the invariant
552 QPRK motif is shown. **(E)** Steady-state kinetic analyses comparing wild-type ScCdc14 and QPRK motif
553 mutants towards pNPP; k_{cat} values were 0.02 (1-449^{QARA}) and 0.03 (1-449^{APRK}) sec⁻¹. **(F)** Same as (E)
554 with the phosphopeptide substrate; k_{cat} values were 0.02 (1-449^{QARA}) and 0.03 (1-449^{APRK}) sec⁻¹. The
555 ScCdc14(1-449) data in panels E and F are identical to panel C. All kinetic data in panels B, C, E, and F
556 are averages of at least 3 independent trials with standard deviation error bars. Fit lines and k_{cat} values
557 were generated in GraphPad Prism using the Michaelis-Menten function.

558 **Figure 2. QPRK mutation causes sensitivity to cell wall stress in *S. cerevisiae*. (A-E)** Cultures of the
559 indicated *S. cerevisiae* strains were serially diluted and spotted on YPAD agar plates containing indicated
560 concentrations of **(A)** methyl methanesulfonate (MMS), **(B)** calcofluor white (CFW), **(C)** micafungin
561 (MF), **(D)** caspofungin (CF), and **(E)** MF or MF + sorbitol. “#1” and “#2” refer to independent isolates of
562 *cdc14^{hm}*. *yen1Δ mus81Δ* is a positive control for MMS sensitivity (87). All plates were incubated at 30°C
563 for 72 hours. Images are representative of three biological replicates. “Wild-type” is W303. **(F)**
564 Immunoblot detecting phosphorylated, active form of Slt2 (pSlt2) from cell lysates of mid-log phase cells
565 with anti-p44/42 MAP kinase antibody. pSlt2 signals were corrected based on the G6PDH (glucose-6-

566 phosphate dehydrogenase) load control and then normalized to the untreated wild-type sample to generate
567 the Relative pSlt2 value, which is an average of two independent trials.

568 **Figure 3. Cdc14-dependent cell wall stress sensitivity is conserved in other fungal species.** Liquid
569 cultures of the indicated *S. pombe* (A) and *C. albicans* (B) strains were serially diluted and spotted on
570 YES or YPD agar plates, respectively, containing the indicated concentrations of micafungin (MF),
571 caspofungin (CF), or calcofluor white (CFW). *CLP1* is the *S. pombe* homolog of *CDC14*. (C) Steady-
572 state kinetic analysis of CaCdc14(1-427) and CaCdc14(1-427^{AARA}) using the Yen1 phosphopeptide
573 substrate. k_{cat} values were 0.092 (1-427) and 0.015 (1-427^{AARA}) sec⁻¹. Data are means from three
574 independent trials and error bars are standard deviations. Liquid cultures of the indicated *C. albicans*
575 strains were serially diluted and spotted on YPD agar plates containing the indicated concentrations of
576 micafungin (D) or caspofungin (E). Plates were incubated at 30 °C for 3-5 days (until mature colonies
577 were visible in the wild-type strain). Images are representative of three independent trials.

578 **Figure 4. Reduced Cdc14 activity causes elevated CWI signaling and perturbs cell wall gene
579 expression in *C. albicans*.** (A) Phosphorylation of Mkc1 (pMkc1) was detected in whole cell extracts
580 from mid-log phase cultures of the indicated *C. albicans* strains by anti-p44/p42 MAP kinase
581 immunoblotting. Saturated cultures were back-diluted to OD₆₀₀ = 0.01 and grown to mid-log phase. A
582 portion of the untreated culture was collected and the remainder was treated with 50 ng/mL micafungin
583 (MF) for 30 min. anti-PSTAIR is a loading control. (B) pMkc1 chemiluminescence signals from (A) were
584 normalized to PSTAIR and plotted as a fold-increase above the untreated wild-type signal. Values are
585 means from three independent experiments and error bars are standard deviations. Unpaired T-tests
586 assuming equal variance comparing pMkc1 level in each strain to wild-type were used to determine
587 statistical significance - * = $p < 0.05$; ns = not significant ($p > 0.05$). (C-F) Relative mRNA levels of
588 selected cell wall stress-responsive genes in mid-log phase cultures of *C. albicans* strains either untreated
589 (-) or treated (+) with 50 ng/mL MF for 1 h were measured by qRT-PCR. Transcript levels were
590 normalized to *RDN18* and set relative to the untreated wild-type sample. Data are averages of at least 5

591 biological trials and error bars are standard deviations. Outliers were identified by Grubbs test and
592 removed if detected. Unpaired T-tests assuming equal variance were used to compare 1) the basal
593 (untreated) expression in each strain with wild-type ($\dagger = p < 0.05$) and 2) untreated with MF-treated
594 samples of each strain. If a significant increase was observed with MF treatment, then the average fold-
595 increase was added above the bar and an additional T-test was performed to determine if fold-increase
596 was significantly different than wild-type fold-increase ($* = p < 0.05$). ns = not significant ($p > 0.05$).

597 **Figure 5. Reduced Cdc14 activity impairs *C. albicans* septum assembly and cell separation. (A-D)**
598 Transmission electron micrographs of *C. albicans* yeast form cells of the indicated strains undergoing
599 septation in mid-log phase liquid cultures. PS = primary septum, SS = secondary septum. (E) Differential
600 interference contrast (DIC) microscopy images of log phase cultures of the indicated strains.

601 **Figure 6. Reduced Cdc14 activity impairs hyphal development on solid medium. (A)** The indicated
602 *C. albicans* strains were grown on Spider medium agar plates at 37 °C for 5 days. Plates were imaged
603 before and after vigorous washing of unattached cells off the surface with water. After washing, agar plus
604 were removed and cross sections were imaged to illustrate depth of invasive growth. (B) Pieces of the
605 agar plugs from (A) were manually ground into small pieces, which were then mounted on a microscopy
606 slide, compressed under a cover slip, and images of embedded cells captured by DIC microscopy.

607 **Figure 7. Loss or reduction of Cdc14 function impairs pathogenesis of *C. albicans*. (A)** *G. mellonella*
608 larvae or (B) immunosuppressed BALB/c mice were infected with 2×10^5 or 5×10^5 *C. albicans* cells of
609 the indicated strains, respectively, or mock-uninfected. p values were determined using a log-rank
610 (Mantel-Cox) test comparing the survival distribution of hosts infected with wild-type *C. albicans* to each
611 experimental strain. (C-E) Histopathological analysis of tissue sections from mouse organs harvested
612 after completion of experiment in (B). In (C) fungal cells were stained with periodic acid-Schiff (PAS) in
613 representative tissue sections to illustrate morphology. In (D) and (E) liver and lung tissues, respectively,
614 were stained with H&E. All images were acquired at 200x magnification, except the *CDC14Δ* sample in

615 (D), which was imaged at 20x to illustrate the necrotic lesion with surrounding inflammation. The
616 *cdc14Δ/Δ* liver section in (D) illustrates one of the rare lesions (associated with the cluster of fungal cells
617 shown in (C)) found in mice infected with *cdc14* mutant strains. In (D) and (E) the following shock-
618 related lesions (lacking invading fungal cells) in mice infected with *CDC14/CDC14* and *CDC14Δ* strains
619 are labeled: endothelial leakage characterized by hepatic (D) or pulmonary alveolar (E) edema (a),
620 multifocal hemorrhage and congestion (b), and intravascular microthrombi (c). Recruited inflammatory
621 cells (d) and necrotic lesions (e) are also labeled. H&E-stained liver and lung sections of an uninfected
622 mouse can be found in **Fig. S8C** for comparison.

623 **ACKNOWLEDGEMENTS**

624 We thank Dr. Kathleen Gould (Vanderbilt University), Dr. Harry Charbonneau (Purdue University), Dr.
625 Michael Weinreich (Van Andel Research Institute), and Dr. Lorraine Symington (Columbia University)
626 for strains and plasmids. We thank Dr. Chris Gilpin and Laurie Muller of the Purdue Life Sciences
627 Microscopy Facility for assistance preparing TEM samples and collecting TEM data. We also thank the
628 Purdue University Animal Resource Facility and Histology Research laboratory for their contributions to
629 this research.

630 REFERENCES

631 1. Culotti J, Hartwell LH. Genetic control of the cell division cycle in yeast. 3. Seven genes
632 controlling nuclear division. *Exp Cell Res.* 1971 Aug;67(2):389–401.

633 2. Visintin R, Craig K, Hwang ES, Prinz S, Tyers M, Amon A. The phosphatase Cdc14 triggers
634 mitotic exit by reversal of Cdk-dependent phosphorylation. *Mol Cell.* 1998 Dec;2(6):709–18.

635 3. Kerk D, Templeton G, Moorhead GB. Evolutionary radiation pattern of novel protein
636 phosphatases revealed by analysis of protein data from the completely sequenced
637 genomes of humans, green algae, and higher plants. *Plant Physiol.* 2008 Feb;146(2):351–
638 67.

639 4. DeMarco AG, Milholland KL, Pendleton AL, Whitney JJ, Zhu P, Wesenberg DT, et al.
640 Conservation of Cdc14 phosphatase specificity in plant fungal pathogens: implications for
641 antifungal development. *Sci Rep.* 2020 Dec;10(1):12073.

642 5. Ah-Fong AM, Judelson HS. New role for Cdc14 phosphatase: localization to basal bodies in
643 the oomycete *Phytophthora* and its evolutionary coinheritance with eukaryotic flagella. *PLoS*
644 *One.* 2011 Feb 14;6(2):e16725.

645 6. Gray CH, Good VM, Tonks NK, Barford D. The structure of the cell cycle protein Cdc14
646 reveals a proline-directed protein phosphatase. *EMBO J.* 2003 Jul 15;22(14):3524–35.

647 7. Kobayashi J, Matsuura Y. Structure and dimerization of the catalytic domain of the protein
648 phosphatase Cdc14p, a key regulator of mitotic exit in *Saccharomyces cerevisiae*. *Protein*
649 *Sci.* 2017 Jul 30;26(10):2105–12.

650 8. Bremmer SC, Hall H, Martinez JS, Eissler CL, Hinrichsen TH, Rossie S, et al. Cdc14
651 phosphatases preferentially dephosphorylate a subset of cyclin-dependent kinase (Cdk)
652 sites containing phosphoserine. *J Biol Chem.* 2012 Jan 13;287(3):1662–9.

653 9. Li L, Ernsting BR, Wishart MJ, Lohse DL, Dixon JE. A family of putative tumor suppressors
654 is structurally and functionally conserved in humans and yeast. *J Biol Chem.* 1997 Nov
655 21;272(47):29403–6.

656 10. Vázquez-Novelle MD, Esteban V, Bueno A, Sacristán MP. Functional Homology among
657 Human and Fission Yeast Cdc14 Phosphatases. *J Biol Chem.* 2005 Aug 12;280(32):29144–
658 50.

659 11. Taylor GS, Liu Y, Baskerville C, Charbonneau H. The activity of Cdc14p, an oligomeric dual
660 specificity protein phosphatase from *Saccharomyces cerevisiae*, is required for cell cycle
661 progression. *J Biol Chem.* 1997 Sep 19;272(38):24054–63.

662 12. Wang WQ, Bembeneck J, Gee KR, Yu H, Charbonneau H, Zhang ZY. Kinetic and
663 Mechanistic Studies of a Cell Cycle Protein Phosphatase Cdc14. *J Biol Chem.*
664 2004;279(29):10.

665 13. Clement A, Solnica-Krezel L, Gould KL. The Cdc14B phosphatase contributes to
666 ciliogenesis in zebrafish. *Development.* 2011 Jan;138(2):291–302.

667 14. Uddin B, Partscht P, Chen NP, Neuner A, Weiß M, Hardt R, et al. The human phosphatase
668 CDC14A modulates primary cilium length by regulating centrosomal actin nucleation. *EMBO*
669 *Rep.* 2019 Jan 1;20(1):e46544.

670 15. Imtiaz A, Belyantseva IA, Beirl AJ, Fenollar-Ferrer C, Bashir R, Bukhari I, et al. CDC14A
671 phosphatase is essential for hearing and male fertility in mouse and human. *Hum Mol*
672 *Genet.* 2018 Mar 1;27(5):780–98.

673 16. Li C, Melesse M, Zhang S, Hao C, Wang C, Zhang H, et al. FgCDC14 regulates cytokinesis,
674 morphogenesis, and pathogenesis in *Fusarium graminearum*. *Mol Microbiol.* 2015
675 Nov;98(4):770–86.

676 17. Li C, Cao S, Zhang C, Zhang Y, Zhang Q, Xu JR, et al. MoCDC14 is important for septation
677 during conidiation and appressorium formation in *Magnaporthe oryzae*. *Mol Plant Pathol.*
678 2018;19(2):328–40.

679 18. Yang G, Hu Y, Fasoyin OE, Yue Y, Chen L, Qiu Y, et al. The *Aspergillus flavus*
680 phosphatase CDC14 regulates development, aflatoxin biosynthesis and pathogenicity. *Front*
681 *Cell Infect Microbiol.* 2018 May;8(141).

682 19. Wang J, Liu J, Hu Y, Ying SH, Feng MG. Cytokinesis-required Cdc14 is a signaling hub of
683 asexual development and multi-stress tolerance in *Beauveria bassiana*. *Sci Rep.* 2013
684 30/online;3:3086.

685 20. Trautmann S, Wolfe BA, Jorgensen P, Tyers M, Gould KL, McCollum D. Fission yeast
686 Clp1p phosphatase regulates G2/M transition and coordination of cytokinesis with cell cycle
687 progression. *Curr Biol.* 2001 Jun 26;11(12):931–40.

688 21. Cueille N, Salimova E, Esteban V, Blanco M, Moreno S, Bueno A, et al. Flp1, a fission yeast
689 orthologue of the *s. cerevisiae* CDC14 gene, is not required for cyclin degradation or rum1p
690 stabilisation at the end of mitosis. *J Cell Sci.* 2001 Jul;114(Pt 14):2649–64.

691 22. Powers BL, Hall MC. Re-examining the role of Cdc14 phosphatase in reversal of Cdk
692 phosphorylation during mitotic exit. *J Cell Sci.* 2017 Jan 1;jcs.201012.

693 23. Jungbluth M, Renicke C, Taxis C. Targeted protein depletion in *Saccharomyces cerevisiae*
694 by activation of a bidirectional degron. *BMC Syst Biol.* 2010;4:176.

695 24. Taxis C, Stier G, Spadaccini R, Knop M. Efficient protein depletion by genetically controlled
696 deprotection of a dormant N-degron. *Mol Syst Biol.* 2009;5:267.

697 25. Wang M, Herrmann CJ, Simonovic M, Szklarczyk D, Mering C. Version 4.0 of PaxDb:
698 Protein abundance data, integrated across model organisms, tissues, and cell-lines.
699 *Proteomics.* 2015 Sep;15(18):3163–8.

700 26. Manzano-López J, Monje-Casas F. The Multiple Roles of the Cdc14 Phosphatase in Cell
701 Cycle Control. *Int J Mol Sci.* 2020;21(3).

702 27. Clifford DM, Wolfe BA, Roberts-Galbraith RH, McDonald WH, Yates JR, Gould KL. The
703 Clp1/Cdc14 phosphatase contributes to the robustness of cytokinesis by association with
704 anillin-related Mid1. *J Cell Biol.* 2008 Apr 7;181(1):79–88.

705 28. Bembenek J, Kang J, Kurischko C, Li B, Raab JR, Belanger KD, et al. Crm1-mediated
706 nuclear export of Cdc14 is required for the completion of cytokinesis in budding yeast. *Cell
707 Cycle.* 2005 Jul;4(7):961–71.

708 29. Clemente-Blanco A, Gonzalez-Novo A, Machin F, Caballero-Lima D, Aragon L, Sanchez M,
709 et al. The Cdc14p phosphatase affects late cell-cycle events and morphogenesis in *Candida
710 albicans*. *J Cell Sci.* 2006 Mar 15;119(Pt 6):1130–43.

711 30. Manzano-López J, Monje-Casas F. The Multiple Roles of the Cdc14 Phosphatase in Cell
712 Cycle Control. *Int J Mol Sci.* 2020;21(3).

713 31. Brand A. Hyphal growth in human fungal pathogens and its role in virulence. Naglik JR,
714 editor. *Int J Microbiol.* 2011 Nov 9;2012:517529.

715 32. Lo HJ, Köhler JR, DiDomenico B, Loebenberg D, Cacciapuoti A, Fink GR. Nonfilamentous
716 *C. albicans* mutants are avirulent. *Cell.* 1997 Sep 5;90(5):939–49.

717 33. Li Y, Cross FR, Chait BT. Method for identifying phosphorylated substrates of specific
718 cyclin/cyclin-dependent kinase complexes. *Proc Natl Acad Sci U A.* 2014 Aug
719 5;111(31):11323–8.

720 34. Wolfe BA, McDonald WH, Yates JR, Gould KL. Phospho-regulation of the Cdc14/Clp1
721 phosphatase delays late mitotic events in *S. pombe*. *Dev Cell.* 2006 Sep 1;11(3):423–30.

722 35. Taylor GS, Liu Y, Baskerville C, Charbonneau H. The Activity of Cdc14p, an Oligomeric
723 Dual Specificity Protein Phosphatase from *Saccharomyces cerevisiae*, Is Required for Cell
724 Cycle Progression. *J Biol Chem.* 1997 Sep;272(38):24054–63.

725 36. Eissler CL, Mazon G, Powers BL, Savinov SN, Symington LS, Hall MC. The Cdk/Cdc14
726 module controls activation of the Yen1 holliday junction resolvase to promote genome
727 stability. *Mol Cell.* 2014 Apr 10;54(1):80–93.

728 37. Storici F, Resnick MA. The delitto perfetto approach to in vivo site-directed mutagenesis and
729 chromosome rearrangements with synthetic oligonucleotides in yeast. In: *Methods in*
730 *Enzymology* [Internet]. Academic Press; 2006. p. 329–45. Available from:
731 <https://www.sciencedirect.com/science/article/pii/S0076687905090191>

732 38. Breitkreutz A, Choi H, Sharom JR, Boucher L, Neduvu V, Larsen B, et al. A global protein
733 kinase and phosphatase interaction network in yeast. *Science.* 2010 May
734 21;328(5981):1043–6.

735 39. Sucher AJ, Chahine EB, Balcer HE. Echinocandins: the newest class of antifungals. *Ann*
736 *Pharmacother.* 2009 Oct 1;43(10):1647–57.

737 40. Fuchs Beth Burgwyn, Mylonakis Eleftherios. Our paths might cross: the role of the fungal
738 cell wall integrity pathway in stress response and cross talk with other stress response
739 pathways. *Eukaryot Cell.* 2009 Nov 1;8(11):1616–25.

740 41. Torres L, Martín H, García-Saez MI, Arroyo J, Molina M, Sánchez M, et al. A protein kinase
741 gene complements the lytic phenotype of *Saccharomyces cerevisiae* *lyt2* mutants. *Mol*
742 *Microbiol.* 1991 Nov;5(11):2845–54.

743 42. Levin DE. Regulation of cell wall biogenesis in *Saccharomyces cerevisiae*: the cell wall
744 integrity signaling pathway. *Genetics.* 2011;189(4):1145–75.

745 43. Zhao X, Muller EG, Rothstein R. A suppressor of two essential checkpoint genes identifies a
746 novel protein that negatively affects dNTP pools. *Mol Cell.* 1998;2:329–40.

747 44. Mazur P, Morin N, Baginsky W, el-Sherbeini M, Clemas J A, Nielsen J B, et al. Differential
748 expression and function of two homologous subunits of yeast 1,3-beta-D-glucan synthase.
749 *Mol Cell Biol.* 1995 Oct 1;15(10):5671–81.

750 45. Jung US, Levin DE. Genome-wide analysis of gene expression regulated by the yeast cell
751 wall integrity signalling pathway. *Mol Microbiol.* 1999 Dec 1;34(5):1049–57.

752 46. Pérez P, Cortés JCG, Cansado J, Ribas JC. Fission yeast cell wall biosynthesis and cell
753 integrity signalling. *Cell Surf.* 2018 Dec;4:1–9.

754 47. Roemer T, Jiang B, Davison J, Ketela T, Veillette K, Breton A, et al. Large-scale essential
755 gene identification in *Candida albicans* and applications to antifungal drug discovery. *Mol*
756 *Microbiol.* 2003;50(1):167–81.

757 48. Ibe C, Munro CA. Fungal cell wall proteins and signaling pathways form a cytoprotective
758 network to combat stresses. *J Fungi*. 2021;7(9).

759 49. Meitinger F, Pereira G. Visualization of cytokinesis events in budding yeast by transmission
760 electron microscopy. In: Sanchez-Diaz A, Perez P, editors. *Yeast Cytokinesis: Methods and*
761 *Protocols* [Internet]. New York, NY: Springer New York; 2016. p. 87–95. Available from:
762 https://doi.org/10.1007/978-1-4939-3145-3_7

763 50. Walker LA, Lenardon MD, Preechasuth K, Munro CA, Gow NAR. Cell wall stress induces
764 alternative fungal cytokinesis and septation strategies. *J Cell Sci*. 2013 Jun
765 15;126(12):2668–77.

766 51. Fuchs BB, O'Brien E, El Khoury JB, Mylonakis E. Methods for using *Galleria mellonella* as a
767 model host to study fungal pathogenesis. *Virulence*. 2010 Nov 1;1(6):475–82.

768 52. Cotter G, Doyle S, Kavanagh K. Development of an insect model for the in vivo
769 pathogenicity testing of yeasts. *Pathog Dis*. 2000;27(2):163–9.

770 53. Segal E, Frenkel M. Experimental in vivo models of candidiasis. *J Fungi*. 2018;4(1).

771 54. MacCallum DM. Hosting infection: experimental models to assay *Candida* virulence. Tavanti
772 A, editor. *Int J Microbiol*. 2011 Dec 22;2012:363764.

773 55. Hohl TM. Overview of vertebrate animal models of fungal infection. *J Immunol Methods*.
774 2014 Aug 1;410:100–12.

775 56. Chin CF, Bennett AM, Ma WK, Hall MC, Yeong FM. Dependence of Chs2 ER export on
776 dephosphorylation by cytoplasmic Cdc14 ensures that septum formation follows mitosis.
777 Lew D, editor. *Mol Biol Cell*. 2012 Jan;23(1):45–58.

778 57. Miller DP, Hall H, Chaparian R, Mara M, Mueller A, Hall MC, et al. Dephosphorylation of
779 Iqg1 by Cdc14 regulates cytokinesis in budding yeast. *Mol Biol Cell*. 2015 Aug
780 15;26(16):2913–26.

781 58. Foltman M, Molist I, Arcones I, Sacristan C, Filali-Mouncef Y, Roncero C, et al. Ingression
782 progression complexes control extracellular matrix remodelling during cytokinesis in budding
783 yeast. *PLoS Genet*. 2016;12(2):e1005864.

784 59. Palani S, Meitinger F, Boehm ME, Lehmann WD, Pereira G. Cdc14-dependent
785 dephosphorylation of Inn1 contributes to Inn1-Cyk3 complex formation. *J Cell Sci*. 2012 Mar
786 27;

787 60. Meitinger F, Petrova B, Lombardi IM, Bertazzi DT, Hub B, Zentgraf H, et al. Targeted
788 localization of Inn1, Cyk3 and Chs2 by the mitotic-exit network regulates cytokinesis in
789 budding yeast. *J Cell Sci*. 2010 Jun 1;123(Pt 11):1851–61.

790 61. Brace J, Hsu J, Weiss EL. Mitotic exit control of the *Saccharomyces cerevisiae* Ndr/LATS
791 kinase Cbk1 regulates daughter cell separation after cytokinesis. *Mol Cell Biol*. 2011
792 Feb;31(4):721–35.

793 62. Powers BL, Hall H, Charbonneau H, Hall MC. A Substrate Trapping Method for Identification
794 of Direct Cdc14 Phosphatase Targets. *Methods Mol Biol*. 2017;1505:119–32.

795 63. Broadus MR, Gould KL. Multiple protein kinases influence the redistribution of fission yeast
796 Clp1/Cdc14 phosphatase upon genotoxic stress. *Mol Biol Cell*. 2012 Oct;23(20):4118–28.

797 64. Villoria MT, Ramos F, Duenas E, Faull P, Cutillas PR, Clemente-Blanco A. Stabilization of
798 the metaphase spindle by Cdc14 is required for recombinational DNA repair. *EMBO J*. 2017
799 Jan 4;36(1):79–101.

800 65. Diaz-Cuervo H, Bueno A. Cds1 controls the release of Cdc14-like phosphatase Flp1 from
801 the nucleolus to drive full activation of the checkpoint response to replication stress in fission
802 yeast. *Mol Biol Cell*. 2008 Jun;19(6):2488–99.

803 66. Chasman D, Ho YH, Berry DB, Nemec CM, MacGilvray ME, Hose J, et al. Pathway
804 connectivity and signaling coordination in the yeast stress-activated signaling network. *Mol*
805 *Syst Biol*. 2014 Nov 19;10(11):759.

806 67. Tognetti S, Jimenez J, Vigano M, Duch A, Queralt E, de Nadal E, et al. Hog1 activation
807 delays mitotic exit via phosphorylation of Net1. *Proc Natl Acad Sci U A*. 2020 Apr
808 21;117(16):8924–33.

809 68. Sanchez-Diaz A, Nkosi PJ, Murray S, Labib K. The Mitotic Exit Network and Cdc14
810 phosphatase initiate cytokinesis by counteracting CDK phosphorylations and blocking
811 polarised growth. *EMBO J*. 2012 Aug 29;31(17):3620–34.

812 69. López-Avilés S, Kapuy O, Novák B, Uhlmann F. Irreversibility of mitotic exit is the
813 consequence of systems-level feedback. *Nature*. 2009 May 1;459(7246):592–5.

814 70. Kataria M, Mouilleron S, Seo MH, Corbi-Verge C, Kim PM, Uhlmann F. A PxL motif
815 promotes timely cell cycle substrate dephosphorylation by the Cdc14 phosphatase. *Nat*
816 *Struct Mol Biol*. 2018 Dec;25(12):1093–102.

817 71. Kuilman T, Maiolica A, Godfrey M, Scheidel N, Aebersold R, Uhlmann F. Identification of
818 Cdk targets that control cytokinesis. *EMBO J*. 2015 Jan 2;34(1):81–96.

819 72. Chen JS, Broadus MR, McLean JR, Feoktistova A, Ren L, Gould KL. Comprehensive
820 proteomics analysis reveals new substrates and regulators of the fission yeast clp1/cdc14
821 phosphatase. *Mol Cell Proteomics*. 2013 May;12(5):1074–86.

822 73. Meitinger F, Palani S, Pereira G. The power of MEN in cytokinesis. *Cell Cycle*. 2012 Jan
823 15;11(2):219–28.

824 74. Mocciaro A, Schiebel E. Cdc14: a highly conserved family of phosphatases with non-
825 conserved functions? *J Cell Sci*. 2010 Sep 1;123(17):2867–76.

826 75. Kaneva IN, Sudbery IM, Dickman MJ, Sudbery PE. Proteins that physically interact with the
827 phosphatase Cdc14 in *Candida albicans* have diverse roles in the cell cycle. *Sci Rep*. 2019
828 Apr 18;9(1):6258.

829 76. Mocciaro A, Berdugo E, Zeng K, Black E, Vagnarelli P, Earnshaw W, et al. Vertebrate cells
830 genetically deficient for Cdc14A or Cdc14B retain DNA damage checkpoint proficiency but
831 are impaired in DNA repair. *J Cell Biol*. 2010 May 17;189(4):631–9.

832 77. Berdugo E, Nachury MV, Jackson PK, Jallepalli PV. The nucleolar phosphatase *Cdc14B* is
833 dispensable for chromosome segregation and mitotic exit in human cells. *Cell Cycle*. 2008
834 May;7(9):1184–90.

835 78. Saito RM, Perreault A, Peach B, Satterlee JS, van den Heuvel S. The CDC-14 phosphatase
836 controls developmental cell-cycle arrest in *C. elegans*. *Nat Cell Biol*. 2004 Aug 1;6(8):777–
837 83.

838 79. Fonzi WA, Irwin MY. Isogenic strain construction and gene mapping in *Candida albicans*.
839 *Genetics*. 1993 Jul 1;134(3):717–28.

840 80. Gola S, Martin R, Walther A, Dünkler A, Wendland J. New modules for PCR-based gene
841 targeting in *Candida albicans*: rapid and efficient gene targeting using 100 bp of flanking
842 homology region. *Yeast*. 2003 Dec 1;20(16):1339–47.

843 81. Kushnirov VV. Rapid and reliable protein extraction from yeast. *Yeast*. 2000 Jun
844 30;16(9):857–60.

845 82. von der Haar T. Optimized protein extraction for quantitative proteomics of yeasts. *PLOS*
846 *ONE*. 2007 Oct 24;2(10):e1078.

847 83. Baker KM, Hoda S, Saha D, Gregor JB, Georgescu L, Serratore ND, et al. The Set1 Histone
848 H3K4 Methyltransferase Contributes to Azole Susceptibility in a Species-Specific Manner by
849 Differentially Altering the Expression of Drug Efflux Pumps and the Ergosterol Gene
850 Pathway. *Antimicrob Agents Chemother*. 2022;66(5):20.

851 84. Serratore ND, Baker KM, Macadlo LA, Gress AR, Powers BL, Atallah N, et al. A novel
852 sterol-signaling pathway governs azole antifungal drug resistance and hypoxic gene
853 repression in *Saccharomyces cerevisiae*. *Genetics*. 2018 Mar;208(3):1037–55.

854 85. Ames L, Duxbury S, Pawlowska B, Ho H lui, Haynes K, Bates S. *Galleria mellonella* as a
855 host model to study *Candida glabrata* virulence and antifungal efficacy. *Virulence*. 2017 Nov
856 17;8(8):1909–17.

857 86. Wright R. Transmission electron microscopy of yeast. *Microsc Res Tech*. 2000 Dec
858 15;51(6):496–510.

859 87. Ho CK, Mazon G, Lam AF, Symington LS. Mus81 and Yen1 promote reciprocal exchange
860 during mitotic recombination to maintain genome integrity in budding yeast. *Mol Cell*. 2010
861 Dec 22;40(6):988–1000.

862

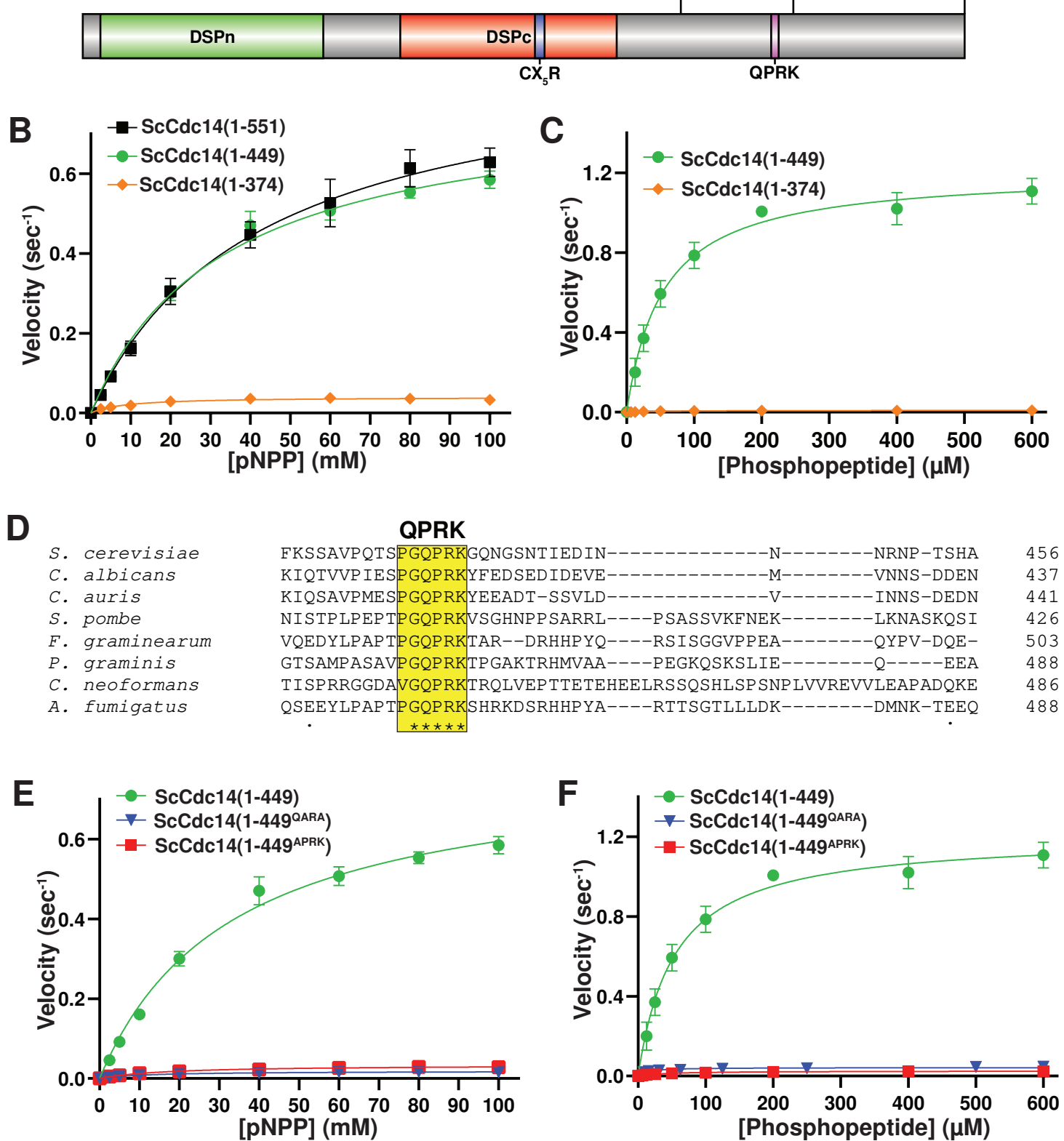


FIGURE 1

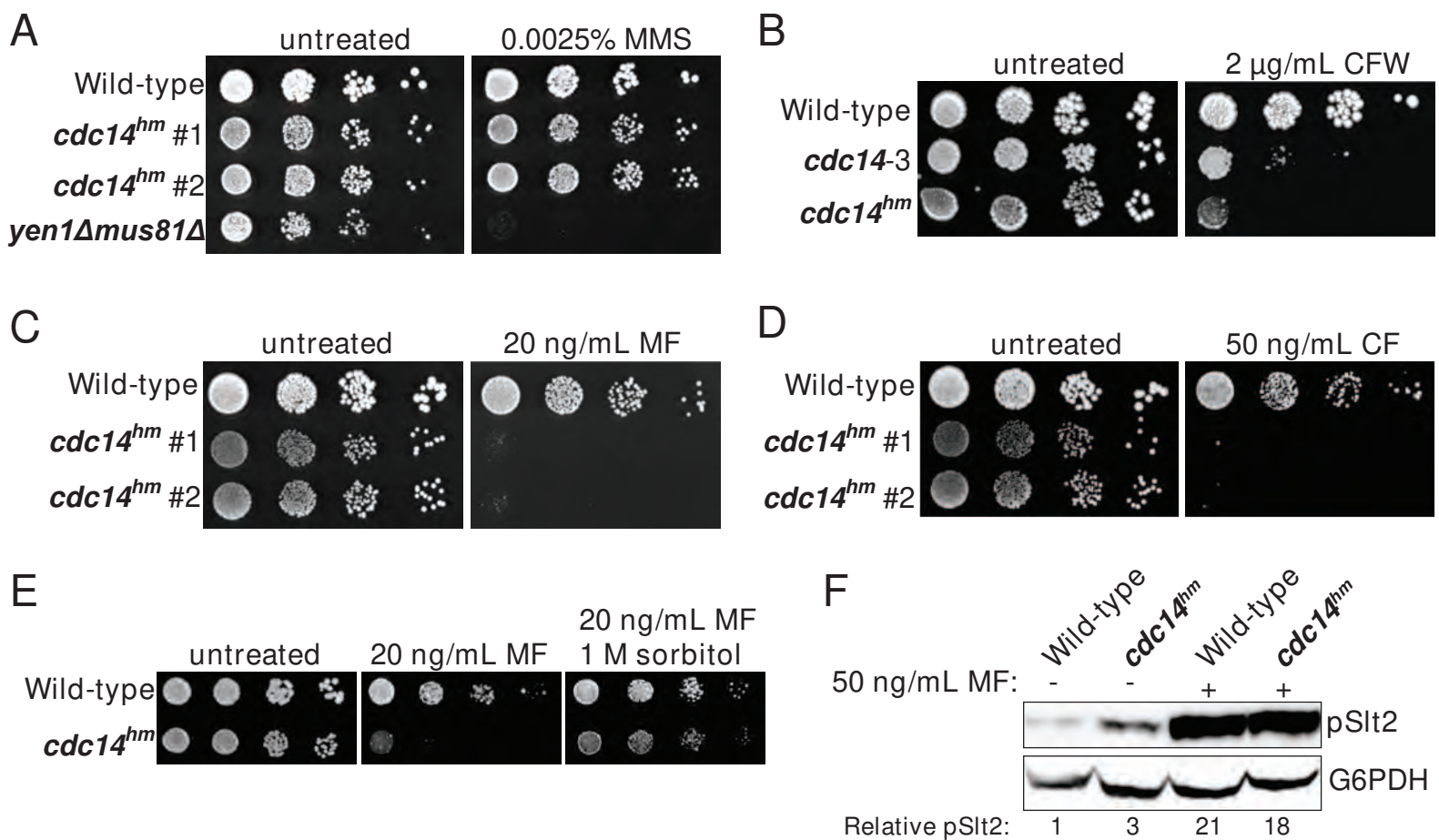


FIGURE 2

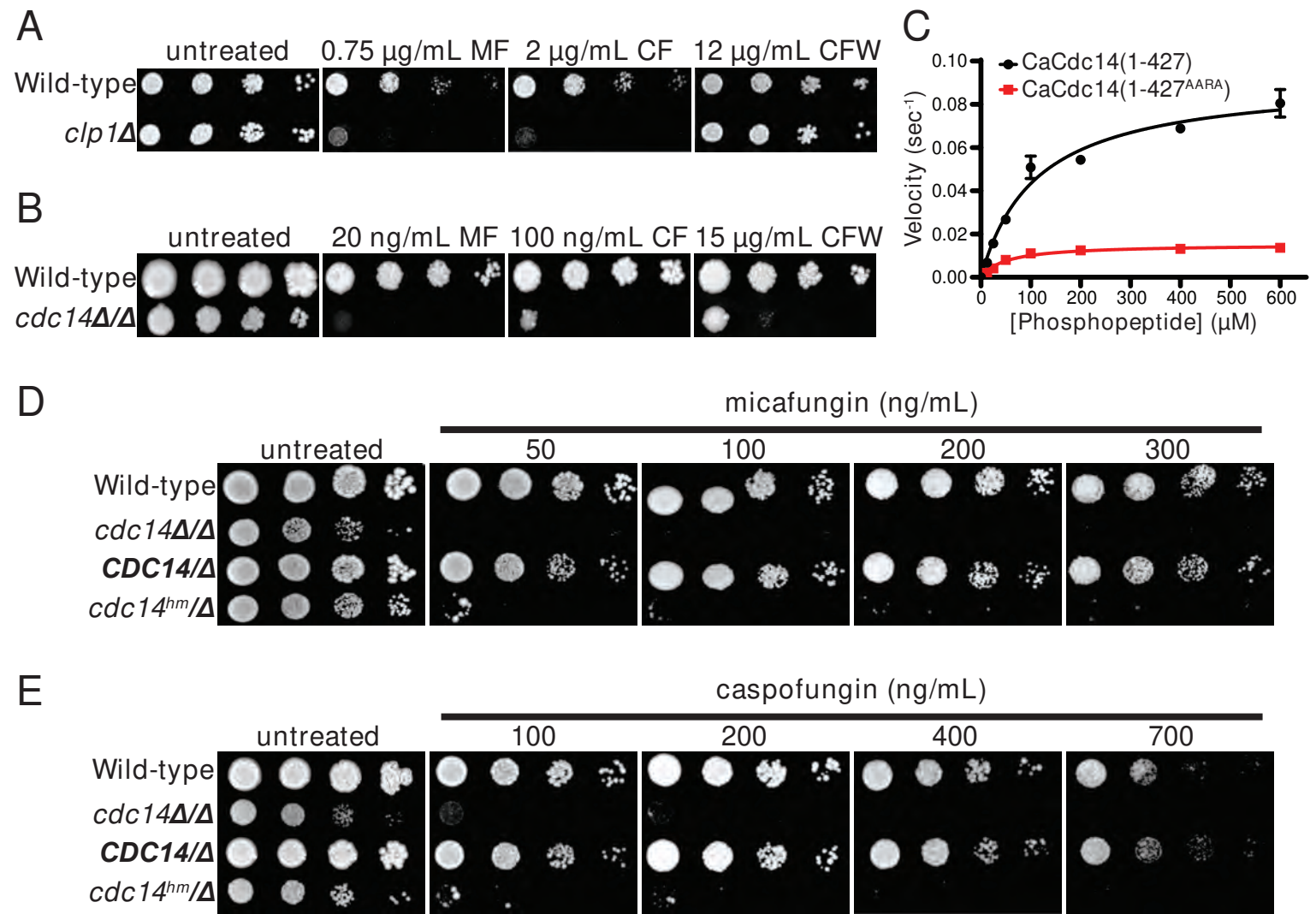
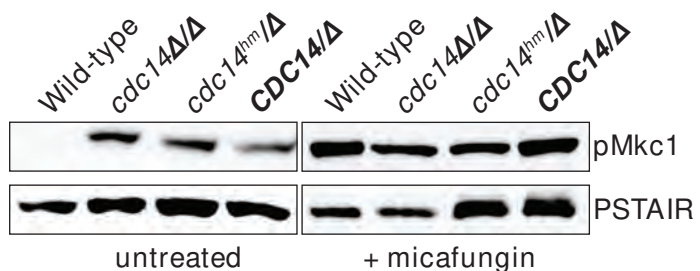
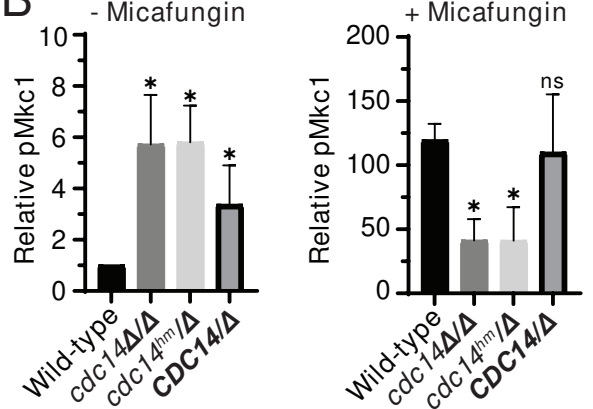


FIGURE 3

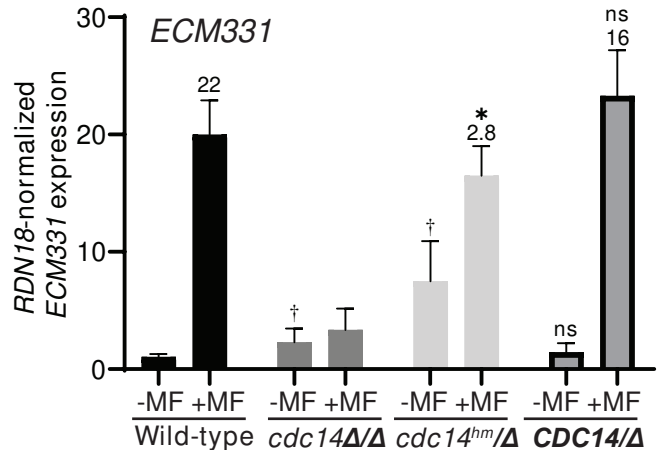
A



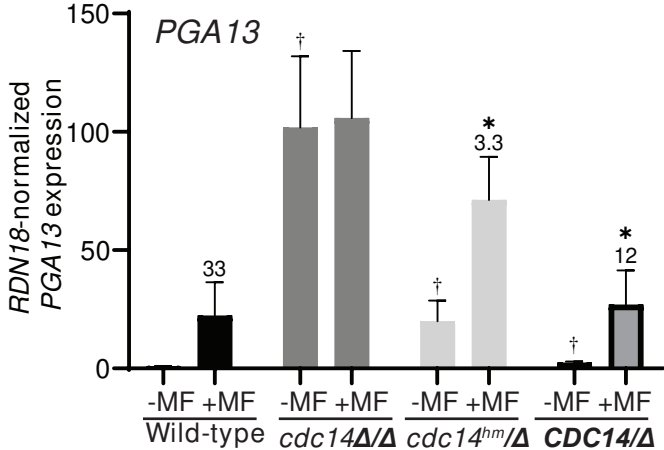
B



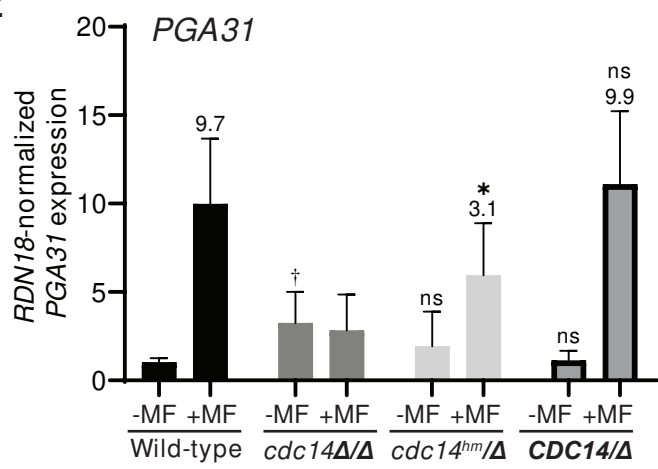
C



D



E



F

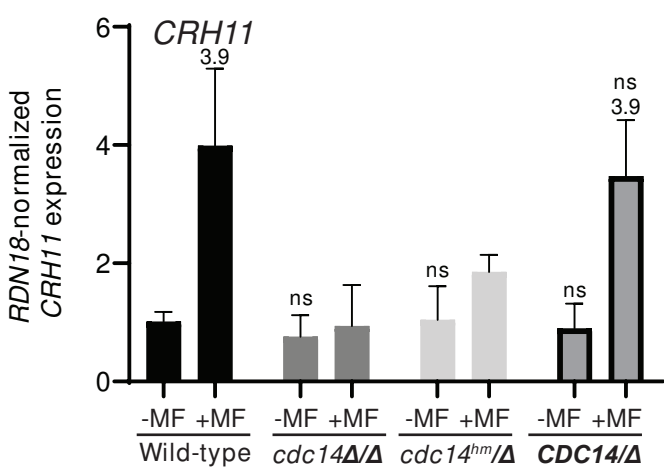


FIGURE 4

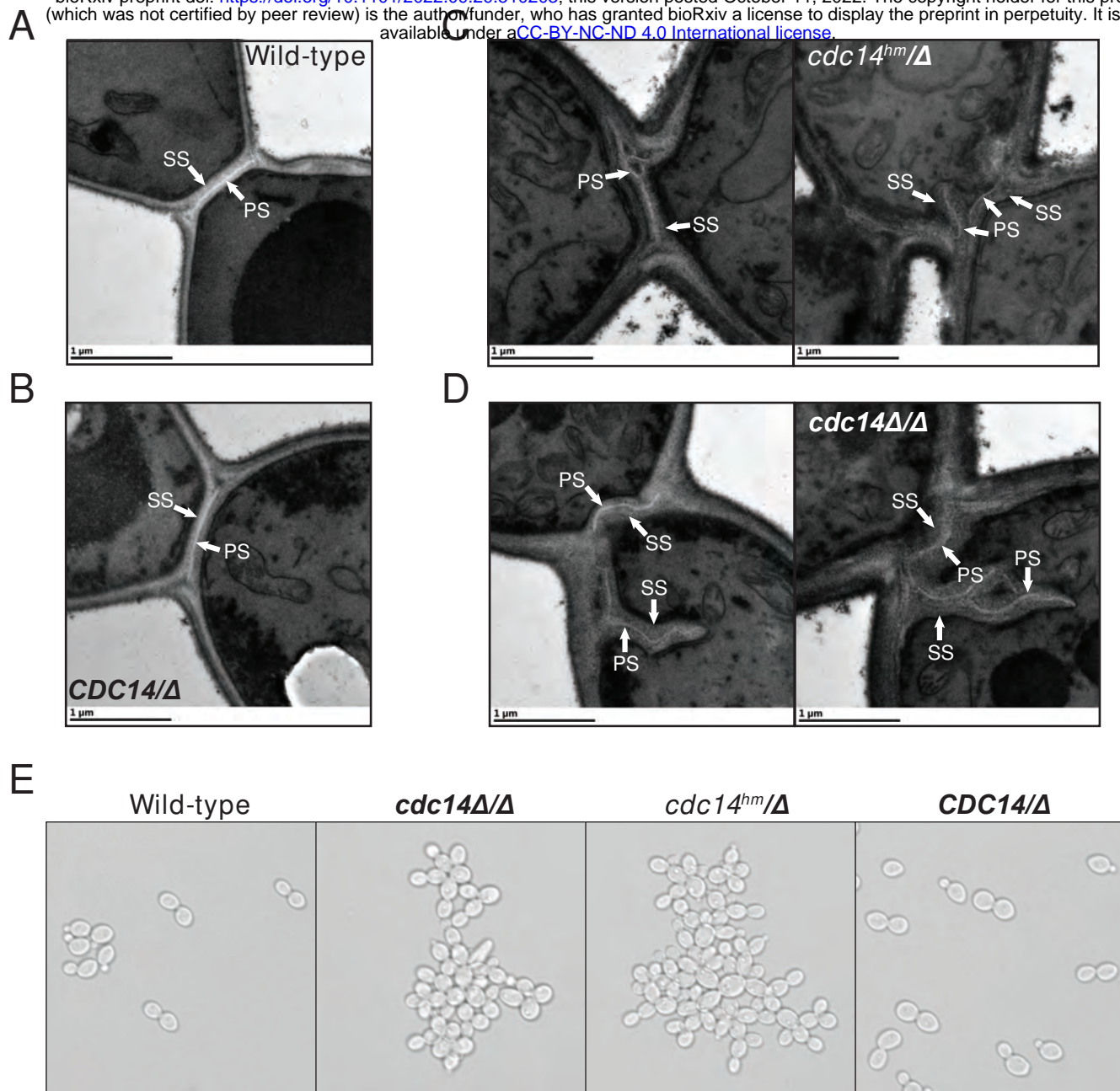


FIGURE 5

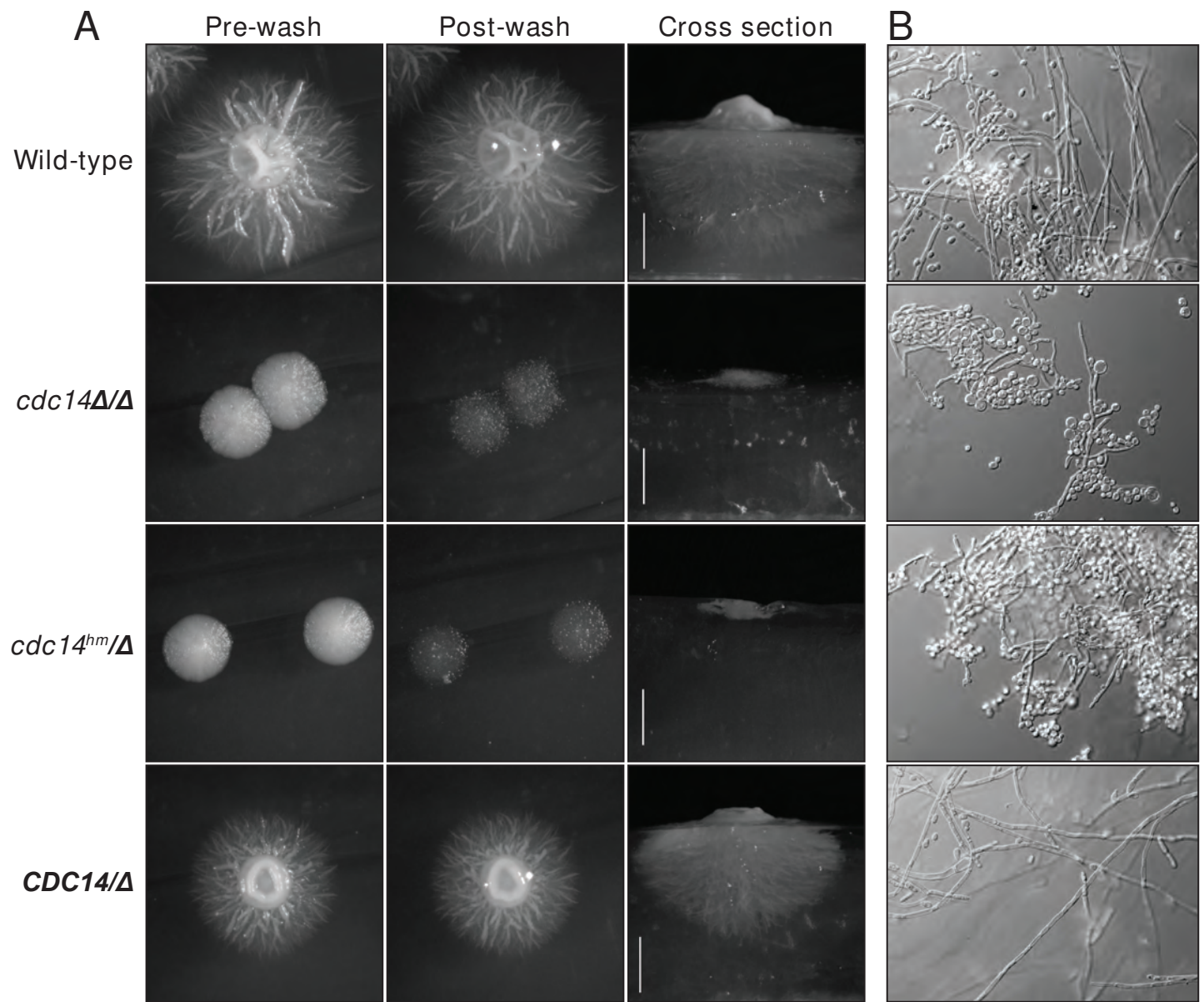
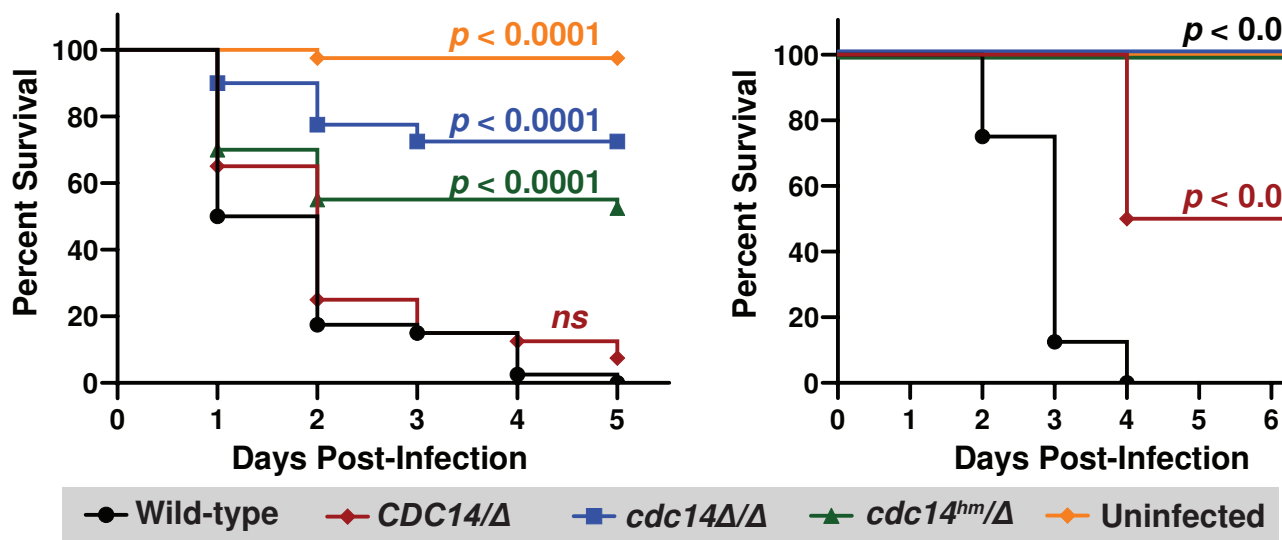
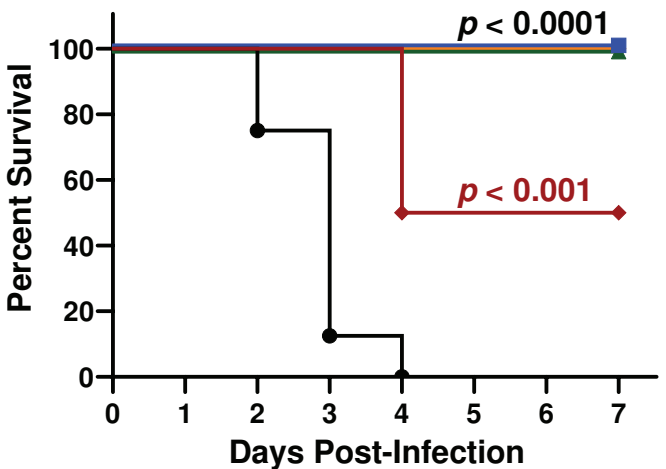


FIGURE 6

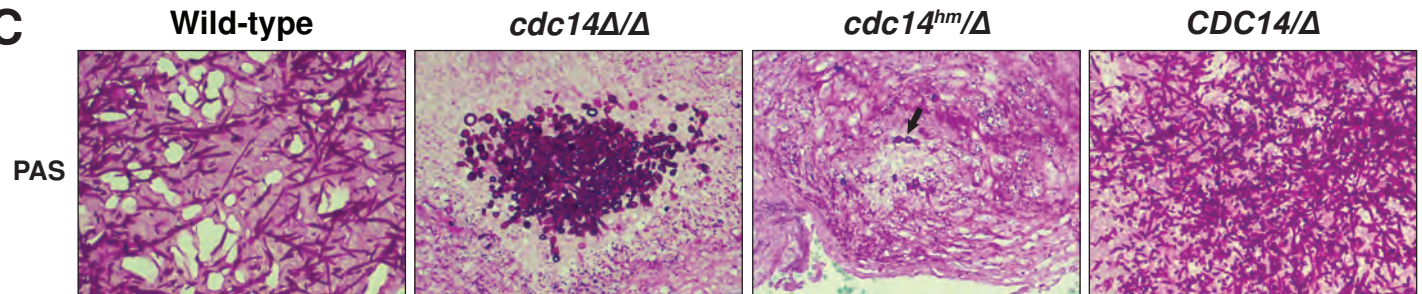
A



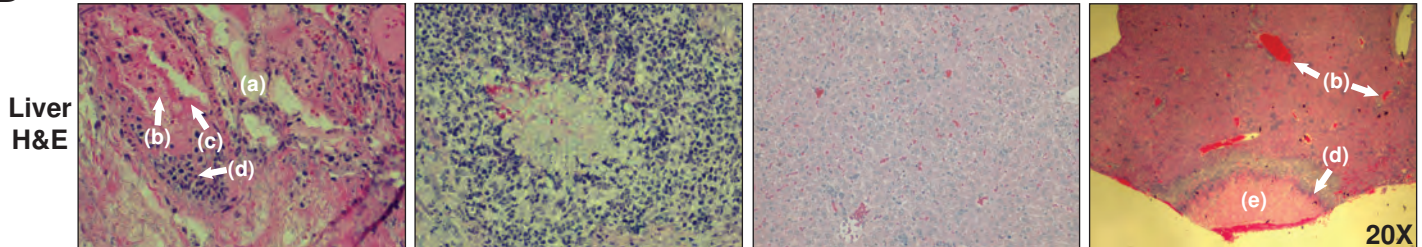
B



C



D



E

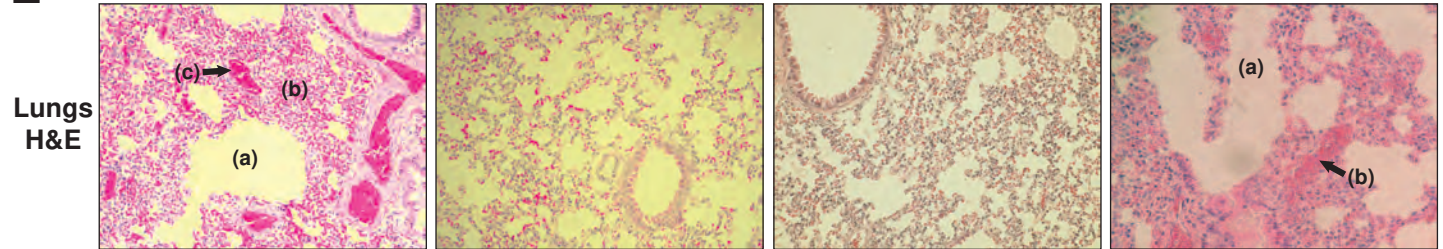


FIGURE 7